FABRICATION AND CHARACTERIZATION OF PHOTONIC CRYSTALS

WANG YANHUA

NATIONAL UNIVERSITY OF SINGAPORE

2005

FABRICATION AND CHARACTERIZATION OF PHOTONIC CRYSTALS

WANG YANHUA

(B. Sc., JILIN UNIVERSITY)

A THESIS SUBMITTED

FOR THE DEGREE OF MASTER OF SCIENCE

DEPARTMENT OF PHYSICS

NATIONAL UNIVERSITY OF SINGAPORE

2005

Acknowledgements

First and foremost, I thank my supervisor, A/Prof. Liu Xiang Yang and co-supervisor, A/Prof. Ji Wei, and Dr. Zhang Keqin for their invaluable guidance and advice throughout my entire candidature in the Department of Physics, National University of Singapore.

I also thank all my group members and friends, Teo Hoon Hwee, Chung Chee Cheong Eric, Dr. Janaky Narayanan, Dr. Strom-Solomonidou, Christina, Dr. Claire Lesieur-Chungkham, Dr. Jiang Huaidong, Dr. Li Jingliang, Dr. Wang Rongyao, Dr. Du Ning, Zhang Jing, Jia Yanwei, Xiong Junying, Zhou Kun, Li Huiping, Zhang Tianhui, Liu Yu, Liu Junfeng, Lim Fung Chye Perry, Pan Hui, Zhang Jie, Liu Yan, Dr. Hendry Izaac Elim, Qu Yingli, Dr. Yu Mingbin (IME) and Dr. Akhmad Herman Yuwono (Material Science), for their cooperation, valuable discussion and help.

Particularly, I should thank my husband, Zheng Yuebing, for his everlasting support and love.

Last but not least, I thank my parents for their support, tolerance, and love.

Table of Contents

Summary

Photonic bandgap (PBG) crystals have attracted great attention because of their potential applications in confining and controlling electromagnetic waves in all three directions of space. Three-dimensional colloidal crystals formed from monodisperse particles possess photonic stop bandgaps. One of the promising methods of fabricating photonic crystals with complete photonic bandgaps is to fill the voids in three-dimensional colloidal crystals with materials possessing high refractive index followed by the removal of the original colloidal crystals.

Although the photonic crystals fabricated from the colloids are studied intensively recently, some bottlenecks exist, for example, defects, disorders and cracks formed invariably in the crystals. Investigations related to the array fashion of the particles and studies on the control of the photonic properties of colloidal crystals are very limited. In our project, we obtained photonic crystals with limited cracks by optimizing fabrication conditions. The effect of surfactants on the array fashion of the particles was investigated systematically, which give a feasible way to improve the fabrication of photonic crystals with controlled crystallography orientations. Furthermore, a novel method is explored to achieve the fine tuning of the photonic crystals. Using colloidal crystal templating, TiO_2 photonic crystals were produced and characterized.

Firstly, the colloidal crystals were fabricated from polystyrene and silica colloidal particles by sedimentation and vertical deposition. The crystals having structure of face centered cubic (fcc) lattice resulted from evaporation-induced interfacial self-assembly crystallization. Through optimizing the fabrication conditions in terms of crystallizing temperature and the concentration of the colloids, the defects, disorders and cracks in the colloidal crystals are greatly reduced and the typical size of a single crystalline domain is larger than 200μm. Their reflectance spectra measured with UV-Vis spectrometer show that they possess photonic stop bandgaps.

Secondly, the effect of surfactants on the structures of polystyrene colloidal crystals was investigated by fabricating colloidal crystals in the presence of different surfactants with different concentrations by sedimentation. The addition of surfactants affected the array fashion and was favorable to form a square array.

Thirdly, the effect of pre-heating treatment on the photonic bandgap properties of silica colloidal crystals was also explored by heating silica colloids as dry powders at elevated temperatures prior to assembly of colloidal crystals. The reflectance spectra of the resulting crystals showed that the central stop bandgap position of the crystals assembled from heat-treated silica particles first blue shifted and then red shifted with the increasing pre-heating temperature as compared to that of the crystal assembled form original silica particles.

Finally, we fabricated the ordered array of air spheres in titania using colloidal crystal templating method, yielding photonic crystals with a high contrast of the refractive index. Micro-FTIR transmission spectroscopy confirmed the presence of stop bandgaps in them. Additionally, a surfactant, SDS, was added into the infiltration material and the SEM results showed that the addition of SDS might lead to tight coating of TiO_2 on the polystyrene microspheres.

List of Tables

List of Figures

Chapter 1 Introduction

1.1 Research Background

1.1.1 Introduction of Photonic Crystals

Photonic crystals are regular arrays of materials with different refractive indices, which would not permit the propagation of electromagnetic waves in a range of frequencies called the photonic band gap. [1] Figure 1.1 shows the simplest case in which two materials are stacked alternately. The spatial period of the stack is known as the lattice constant, since it corresponds to the lattice of ordinary crystals composed of a regular array of atoms. However, one big difference between them is the scale of the lattice constant. In the case of ordinary crystals, the lattice constant is on the order of angstroms. On the other hand, it is on the order of wavelength of the relevant electromagnetic waves for the photonic crystals. For example, it is about 1 μm or less for visible light, and is about 1 mm for microwaves.

Photonic crystals are classified mainly into three categories, that is, one-dimensional (1D), two-dimensional (2D), and three-dimensional (3D) crystals according to the dimensionality of the stack (see Fig. 1.1). The photonic crystals that work in the microwave and far-infrared regions are relatively easy to fabricate. Those that work in the visible region, especially 3D ones are difficult to fabricate because of their small lattice constants (submicron scale). [2] The first photonic crystal was made by Yablonovitch by

drilling three sets of cylindrical holes in a block of dielectric materials in a periodic arrangement.[3] The periodicity was on the order of a millimeter so that the photonic band gap appeared at microwave frequencies.

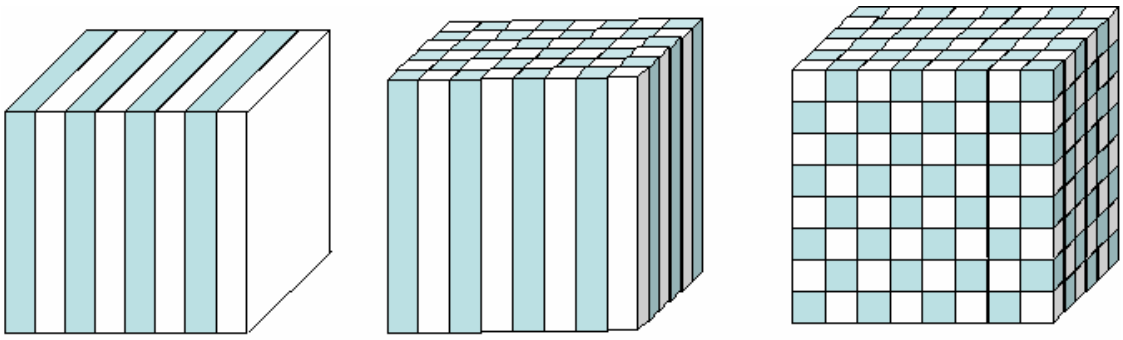

(a) 1 D (b) 2 D (c) 3 D

Figure 1.1. Schematic illustrations of photonic crystals (a) one-dimensional (1D) (b) two-dimensional (2D) (c) three-dimensional (3D)

Photonic crystals can offer us one solution to the problem of optical control and manipulation. If the dielectric constants of the materials in the crystals are different enough, and the absorption of light by the material is minimal, then the scattering at the interfaces can produce many of the same phenomena for photons (light mode) as the atomic potential does for electrons. Light would remain trapped at defect sites if it is forbidden to propagate through the crystals. Such a defect can be shaped in the form of a tiny cavity or a sharply-curved waveguide, allowing one to manipulate light in ways that have not been possible before. Thus, photonic crystals have been proposed for a large number of applications such as efficient microwave antennas, zero-threshold lasers, low-loss resonators, optical switches, and miniature optoelectronic components such as

microlasers and waveguides. The most useful applications would occur at near-infrared or visible wavelengths. This makes it necessary to fabricate photonic crystals with feature sizes of less than a micrometer. Furthermore, the refractive index contrast of the crystal must exceed 2 or 3, depending on the lattice, placing restrictions on the materials used.

A number of different methods have been used for the fabrication of photonic crystals. Many of these apply a variety of lithographic techniques used in the semiconductor industry for patterning substrates such as silicon. Two-dimensional photonic crystals have been made this way, which operate at wavelengths down to the visible light. [4] Good control over the introduction of defects has also been demonstrated. A number of attempts have been made to create three-dimensional photonic crystals using these techniques. [5-7] However, it has so far proved too difficult to achieve submicron periodicities of much more than one unit cell thickness.

On the other hand, colloidal particles naturally possess the desired sizes and can form periodic structures spontaneously. Moreover, the optical properties of the individual spheres can easily be tuned, or they can be used as templates to make inverted structures. Colloidal self-assembly has therefore been proposed as an easy and inexpensive way to fabricate three-dimensional photonic crystals, and as a suitable system in which to investigate their optical properties.[8, 9] Until this realization colloidal crystals had been prepared with only a modest refractive index contrast, in order for them to remain

relatively transparent and not opaque due to multiple scattering. They can thus be said to reject light propagating in certain directions, which satisfy the Bragg condition:

$$2d \sin\theta = m\lambda \quad . \tag{1.1}$$

Here, λ is the wavelength of the incident light on the crystal, d is the lattice spacing, θ is the angle between the incident ray and the lattice planes, and the integer m is the order of the diffraction. If the dielectric contrast between the spheres and the suspending medium is larger, the range of angles for which waves of a given frequency diffracts increases due to multiple scattering. At sufficiently high contrast and for certain crystal types propagation should become impossible in all directions and for both polarizations.

1.1.2 Optical Properties of Photonic Crystals

Propagation of electromagnetic waves in periodic media displays many interesting and useful effects. Shining a light through a large block of glass with a single bubble of air in it, some of it will reflect and some of it will continue forward at a slightly different angle (be refracted). This scattered light allows eyes to see the bubble, perhaps with an attractive sparkling caused by all of the reflections and refractions. Picture now a second bubble in the glass, just like the first but at a different place. As before, the light will reflect and refract, this time from both bubbles, sparkling in a more intricate pattern than before. All of these is exactly predicted by Maxwell's equations. [10] For time-varying fields, the differential form of these equations in cgs units is:

$$\vec{\nabla} \times \vec{E} = -\frac{1}{c}\frac{\partial \vec{H}}{\partial t}, \tag{1.2}$$

$$\vec{\nabla} \times \vec{H} = \frac{4\pi}{c} J + \frac{1}{c}\frac{\partial \varepsilon \vec{E}}{\partial t}, \tag{1.3}$$

$$\vec{\nabla} \cdot \varepsilon \vec{E} = 4\pi\rho, \tag{1.4}$$

$$\vec{\nabla} \cdot \vec{H} = 0, \tag{1.5}$$

Where $\vec{E}$ and $\vec{H}$ are the electric and magnetic fields, J is the free current density, ρ is the free charge density, ε is dielectric constant and c is the speed of light in vacuum.

After a little manipulation, Maxwell's Equations can be reduced to a wave equation of the form:

$$\vec{\nabla} \times \frac{1}{\varepsilon}\vec{\nabla} \times \vec{H} = \left(\frac{\omega}{c}\right)^2 \vec{H} \tag{1.6}$$

This is an eigenproblem for $\vec{H}$, where ω is angular frequency of the wave. It can be shown that the operator acting on the $\vec{H}$ field is Hermitian, and, as a consequence, its eigenvalues are real and positive.

The Bloch-Floquet Theorem tells us that, for a Hermitian eigenproblem whose operators

are periodic functions of position, the solution can always be chosen of the form $e^{i\vec{k}\cdot\vec{x}}\cdot$(periodic function). A periodic function $f(\vec{x})$ is one such that $f(\vec{x}+\vec{R}_i)=f(\vec{x})$ for any $\vec{x}$ and any primitive lattice vector $\vec{R}_i$ of the crystal.

From the Bloch-Floquet Theorem, the solution of Eq. (1.6) for a periodic ε can be chosen of the form:

$$\vec{H}=e^{i(\vec{k}\cdot\vec{x}-\omega t)}\vec{H}_{\vec{k}}, \tag{1.7}$$

Where $\vec{H}_{\vec{k}}$ is a periodic function of position and satisfies the "reduced" Hermitian eigenproblem:

$$(\vec{\nabla}+i\vec{k})\times\frac{1}{\varepsilon}(\vec{\nabla}+i\vec{k})\times\vec{H}_{\vec{k}}=\left(\frac{\omega}{c}\right)^2\vec{H}_{\vec{k}}. \tag{1.8}$$

Because $\vec{H}_{\vec{k}}$ is periodic, this eigenproblem is needed only considered over a finite domain: the unit cell of the periodicity. Eigenproblems with a finite domain have a discrete set of eigenvalues, so the eigenfrequencies ω are a countable sequence of continuous functions: $\omega_n(\vec{k})$ (for n = 1, 2, 3 …). When they are plotted as a function of the wavevector $\vec{k}$, these frequency "bands" form the band structure of the crystal.

Figure 1.2 shows band structure of an 'inverse' face-centered cubic lattice of spheres consisting of air in a background material of refractive index 3. The frequencies of the allowed modes are plotted versus wave vectors in the Brillouin zone of the f.c.c. lattice of

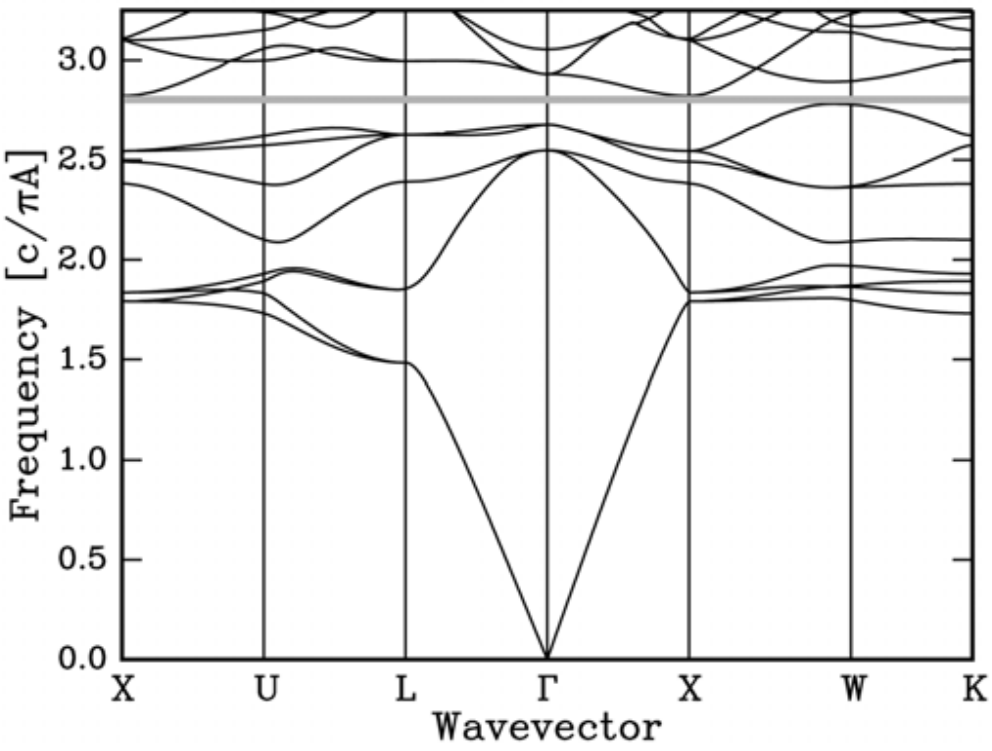

Figure 1.2. Band structure of an 'inverse' fcc lattice of spheres of refractive index 1 in a background with index 3 calculated with the KKR method.[11] The horizontal gray band outlines the complete band gap.

spheres. The allowed modes form the photonic band structure of this crystal. There is a narrow band gap at a frequency of $\nu = 2.8c/\pi A$, where c is the speed of light and A the size of the cubic unit cell. The 'inverted' crystal structure is shown here because the 'direct' structure, i.e. spheres of high refractive index in air, does not possess a band gap.

If the refractive index contrast (the ratio of the refractive index of the spheres and their background) is increased the band gap widens. Below a contrast of 2.85 the gap is closed.[11] The band gap in Figure 1.2 is located between the 8th and 9th bands. This corresponds to the region where, in weakly scattering crystals, the second order Bragg diffraction is located. The first order Bragg diffraction occurs at a lower frequency, around $\nu = 1.7c/\pi A$ for the direction corresponding to the L point. At this point the waves travel perpendicularly to the (111) planes of the crystal. There is a sizeable range of frequencies for which these waves cannot propagate through the crystal and thus are reflected. This frequency range is called a stop bandgap. Since propagation is still possible in other directions one usually speaks of a partial or incomplete band gap. If the direction is moved away from the L or X points the bands are seen to split in two. These are the different polarization states which are then no longer degenerate. There is a close analogy with electron waves traveling in the periodic potential of atomic crystals, where, too, the allowed modes are arranged into energy bands separated by energy gaps.

1.1.3 Optical Characterization

Optical measurements are the main technique for the characterization of photonic band gap materials. While optical reflectance and transmission are the principle tools used to characterize 3D systems. An infinitely large, perfect photonic crystal would reflect 100% of the incident light at wavelengths in the band gap and would transmit 100% of the light

at other wavelengths. At any given angle of incidence there will be such gaps. In the case of a complete band gap the reflected wavelength bands would overlap at every incident angle. However, a number of experimental complications arise in practice. First of all, real photonic crystals are neither perfect nor infinite. This problem is made worse by a certain degree of disorder or the presence of defects, which cause the dip in the transmission to broaden and its edges to become less well defined. Another related problem is polycrystallinity of the sample, which often occurs in self-assembled crystals. This will result in a large broadening of the transmitted and reflected bands, because changing the wavelength will successively probe different crystallites with different orientations. In all these cases, simply taking the full width at half maximum is therefore not necessarily the best way to proceed.

Trying to observe a single crystal with as few defects as possible should be able to minimize these difficulties. Polycrystallinity is not normally a problem in crystals made with lithographic techniques, but may be a limitation in self-assembled crystals. It has been shown that gap widths extracted from reflection spectra are much more reliable than those obtained from transmission spectra, because reflected light probes only a small number of lattice planes lying close to the surface[12] (thus containing fewer domains with limited defects). One should therefore reduce the probe beam to a size smaller than a single crystalline domain. Reducing the beam size even further to much less than the

domain size will further reduce the influence of defects and surface roughness. This was beautifully demonstrated in reflection and luminescence spectra measured with the use of an optical microscope.[13] Alternatively, polycrystallinity can be avoided by growing large single crystals, which are not too thick, so that transmission spectra also produce accurate gap widths.[14, 15]

1.1.4 Fabrication of Photonic Crystals

Numerical calculations have led to the identification of a number of three-dimensional crystal structures that should have a complete photonic band gap. Fabrication of these structures on a submicrometer length scale is still a challenge, especially because materials with a sufficiently high refractive index and negligible absorption have to be used. Suitable materials are often semiconductors such as TiO_2, Si, or GaAs. The structures must also have a very high porosity, typically containing ~80% air. A number of strategies have been developed; generally, they are nanofabrication, self-assembly methods, colloidal crystal templating and directed self-assembly methods.

1.1.4.1 Nanofabrication

Nanofabrication techniques use lithography and etching, or holography. Modern semiconductor processing techniques have so far had relatively limited success in making

three-dimensional structures as compared to their success in the fabrication of two-dimensional photonic crystals. A promising approach is the layer-by-layer preparation of the so-called woodpile structure, which is known to have a complete band gap.[16, 17]

An alternative method is the use of chemically assisted ion beam etching to drill narrow channels into a GaAs or GaAsP wafer[18, 19] in a manner similar to that used by Yablonovitch, but on a much smaller length scale. Photo-assisted electrochemical etching of pre-patterned silicon has been used to produce a two-dimensional array of very deep (~100 μm) cylindrical holes.[20] By modulating the light intensity with time it is possible to induce a periodicity of up to 25 periods in the vertical direction.[21] So far, this periodicity is relatively large as compared to that in the horizontal directions, so that the structure does not yet possess a complete photonic band gap.

The last method mentioned here is three-dimensionally periodic patterns of light created by interfering up to four laser beams,[22, 23] similar to holographic recording. The pattern is recorded in a film of photoresist. Unpolymerized resin is then removed by washing. The method is suitable for quickly producing large-area crystals with any desired structure, as long as the polymerized regions are interconnected. Absorption of the light by the photoresin limits the maximum thickness of the crystals to several tens of micrometers,

corresponding to several tens of lattice planes. Since photoresists have a relatively low refractive index, additional steps must be used to increase the dielectric contrast.

1.1.4.2 Self-Assembly Methods

Monodisperse colloidal particles can spontaneously organize into three-dimensionally periodic crystals with a macroscopic size. Their lattice constant is easily adjusted from the nanometer to the micrometer range by varying the size of the particles. Colloidal crystals form spontaneously if there is a thermodynamic driving force, for example a sufficiently high particle concentration, making it favorable for the particles to order into a lattice, thus using the limited space more efficiently. Typical crystal sizes are from tens to thousands of micrometers. The crystal structure formed usually is face centered cubic (fcc), although low volume fraction body centered cubic (bcc) crystals are formed if the particles interact repulsively over distances much longer than their sizes.[24] Particles which interact nearly as hard spheres show a tendency to form randomly stacked hexagonal layers. In this structure the stacking order of the hexagonally packed (111) planes is not ABCABC… as in fcc, nor ABAB… as in hcp, but close to random.[25, 26]

Their self-organizing properties make spherical colloids as suitable candidates for fabricating photonic crystals. There are only a few materials from which colloids can be made with sufficient monodispersity to crystallize, namely silica, ZnS, and a number of

polymers, most notably polystyrene and polymethylmethacrylate. Most of the colloidal crystals of these materials have a relatively modest refractive index contrast, even when dried.

1.1.4.3 Colloidal Crystal Templating

The early calculations had already shown that the prevailing fcc structure possesses a complete photonic band gap only for the inverted crystal structure, in which the air spheres have a lower index than their environment.[27] Furthermore, the refractive index contrast needs to be very large (>2.85). Although the diamond structure has a complete band gap for the direct crystal structure[28] it is never formed by colloidal self-assembly. More detailed calculations of the photonic properties of crystals formed by self-assembling systems determined that the optimal air filling fraction was around 80%,[29, 30] but did not identify structures that are easier to fabricate. These facts quickly led to the development of chemical means by which the interstitial voids of a colloidal crystal can be filled with a high index solid, after which the colloidal particles can be removed.[31-37] These approaches are known collectively as colloidal crystal templating methods. In that way, the air filling fraction of such an “inverse opal” is automatically close to the maximum sphere packing fraction of 74% and a larger variety of materials can be used.

The initial templating methods used emulsion droplets[31] or polystyrene spheres[33, 35, 37] as the colloidal templates, and sol-gel chemistry to fill the interstitial space. Using emulsion droplets ordered porous materials of titania (TiO_2), zirconia (ZrO_2), silica, and polyacrylamide were made.[31, 32] The emulsion oil droplets are not easy to make monodisperse, but they are easy to remove by dissolution or evaporation. A calcination step then converted the titania gel into the desirable high refractive index titania phases anatase (n=2.5, above 400°C) or rutile (n=2.8, above 900°C).[38] In an independent work polystyrene latex spheres and a sol-gel reaction were used to produce inverted crystals of amorphous silica.[33, 34] Because polystyrene spheres are easy to obtain with high monodispersity and because they self-assemble with great ease they have been used in many subsequent templating studies.[35, 36, 39-42] These particles are removed either by calcination or by dissolution, for example, toluene. Monodisperse polymethylmethacrylate spheres may be used similarly.[43] Silica spheres can be made equally monodisperse as polymer colloids, but must be removed by etching with a hydrogen fluoride (HF) solution.[44-48] All these approaches have resulted in materials containing large domains of well-ordered spherical pores.

Many metal oxides (titania, silica, zirconia, alumina, yttria, etc.) are produced by hydrolysis of the corresponding liquid metal alkoxide, which is infused into the pores by capillary action, sometimes aided by suction.[35-37, 40-42] An alternative approach is to use

ultrafine powders of silica or nanocrystalline rutile, which are added to a monodisperse polystyrene latex. The mixed suspension is then dried slowly to produce an ordered macroporous material in one step.[49-52] Similar approaches using 4 nm CdSe quantum dots and gold nanocrystals[53, 54] have also been used. Due to the small size of the particles efficient pore filling is achieved.

Polymeric inverted opals have been made of polyacrylamide, polystyrene, polymethylmethacrylate, and polyurethane by infiltrating colloidal crystals with a liquid monomer followed by heating or exposure to UV light to initiate the polymerization.[32,55-57]

Precipitation reactions of salts followed by chemical conversion have been applied to expand the variety of accessible materials to a large number of carbonates and oxides of metals which cannot be prepared by sol-gel chemistry.[58]

Electrochemical deposition can also be used to template colloidal crystals that have been deposited on an electrode. Alternatively, opals can be infiltrated with molten metals at increased pressure.[59]

The last templating method is chemical vapor deposition (CVD), with which the degree of filling can be accurately controlled. Thus, CVD was used to fill silica crystals with graphite and diamond, silicon, that has a refractive index of 3.5 and is transparent at wavelengths above 1100 nm,[48] and germanium.[60] A difficulty was the obstruction with material of the outermost channels which provide access to the innermost channels. Using low-pressure CVD, which prevented channel obstruction, and highly ordered silica crystals, inverted crystals of silicon were made.

1.1.4.4 Directed Self-Assembly

Although colloidal self-assembly has distinct advantages in the fabrication of three-dimensional photonic crystals it also has a number of drawbacks. Without gentle persuasion the material formed is polycrystalline, contains lattice defects and stacking errors, and can only form a limited number of crystal structures, which have a random orientation. A number of strategies have been developed to overcome these limitations. Methods in which an external influence is used to direct particles to preferred lattice positions are called directed self-assembly techniques.

A relatively simple technique that already produces well-ordered crystals is called convective self-assembly or vertical deposition. This process is easy to be realized. A clean and flat substrate such as microscope slide is placed vertically in a colloidal

suspension. As the solvent evaporates from the meniscus more particles are transported to the growing film by fluid flow. Capillary forces in the drying film pull the spheres into a regular close packing. The number of layers can be controlled accurately by the particle volume fraction. The resulting crystal has a uniform orientation over centimeter distances, making it essentially single-domain. Although vacancies exist their number is relatively small. Cracks often form during drying but the crystal orientation is preserved across cracks. Sedimentation of particles larger than about 0.5 μm prevents their deposition in this way. However, this problem can be overcome by applying a temperature gradient which causes a convective flow counteracting sedimentation. Vertical deposition has produced some of the best ordered colloidal crystals, which are suitable for investigating the optical properties of photonic crystals, both the direct and inverted structures.[61, 62]

Another approach of formation of well-ordered, large-area crystals of close-packed spheres is to filter colloidal spheres into a thin slit between two parallel plates.[63-65] The crystal thickness can be controlled from a monolayer to several hundreds of layers through the plate separation. Fabrication of the filter cells uses photolithography and cleanroom facilities, but an easier method has been developed using replica molding against an elastomeric mold.[66] Long-range fcc order has also been induced by applying shear flow to a concentrated colloidal suspension enclosed between parallel plates.[67]

Although electrophoretic deposition is widely used for the deposition of particulate films of many different materials it can also be used to prepare ordered three-dimensional sphere packings.[68-71] The quality of the crystals formed appears to be comparable to that obtained by sedimentation, but is somewhat lower than that in crystals formed by vertical deposition. It is much faster, though.

The methods to direct colloidal self-assembly mentioned so far produce (nearly) close packed crystals of the fcc type. Their (111) planes are always arranged parallel to the substrate. Other directed self-assembly methods try to overcome these limitations.

In colloidal epitaxy the colloidal particles sediment onto a substrate that has been patterned lithographically with a regular array of pits roughly half a particle deep.[72,73] The first particles fall into the pits, providing a template for other particles. When the first layer was forced to be a (100) or (110) lattice plane of fcc this orientation of the growing crystal was preserved over thousands of layers with relatively few defects. Colloidal crystals can also form binary crystals if the size ratio between the two types of spheres is carefully adjusted.

Different crystal structures can also be made by making the interaction potential between

the colloidal spheres anisotropic. For example, dipolar interactions can be induced by applying a high-frequency electric field. This results in self-assembly of a body-centered tetragonal crystal structure.[74] Using optical tweezers or other more advanced techniques of single-particle manipulation it should be possible to build many more crystal structures.

1.2 Objectives

The first objective of this project is to fabricate high-quality colloidal photonic crystals with less defects, cracks and large single crystal domains by sedimentation and modified vertical deposition.

The second objective is to investigate the effects of surfactants on the array fashion of the particles.

The third one is to explore the effects of pre-heating treatment on the photonic bandgap properties of colloidal photonic crystals.

The last one is to fabricate surfactant-assisted TiO_2 photonic crystals using colloidal crystal templating and to prove their stop bandgaps by optical characterization.

1.3 Organization of the Thesis

This thesis is structured as follows. The first chapter serves as introduction of the basics, the optical properties and the fabrication of photonic crystals, as well as the objectives and organization of this project. It will also deal with the main techniques of characterization. The second chapter is devoted to fabrication and characterization of colloidal crystals as three-dimensional photonic crystals. The effects of surfactants on the structure of polystyrene colloidal crystals and the effects of pre-heating treatment on the photonic bandgap properties of silica colloidal crystals will be described in the third and the fourth chapters, respectively. Fabrication of well ordered TiO_2 photonic crystals with large single domain by the methods of colloidal crystal templating will be included in the fifth chapter. The last chapter is conclusion.

References

[1] Arnout Imhof, *Three-Dimensional Photonic Crystals Made from Colloids*, 424-446

[2] Kazuaki Sakoda, *Optical Properties of Photonic Crystals*, Springer, 2-3

[3] E. Yablonovitch, T. J. Gmitter, and K. M. Leung, *Phys. Rev. Lett.* **67**, 2295-2298 (1991).

[4] C. M. Soukoulis (Ed.), *Photonic Crystals and Light Localization in the 21st Century* (Kluwer Academic, Dordrecht, The Netherlands, 2001).

[5] S. Y. Lin, J. G. Fleming, D. L. Hetherington, B. K. Smith, R. Biswas, K. M. Ho, M. M. Sigalas, W. Zubrzycki, S. R. Kurtz, and J. Bur, *Nature* **394**, 251-253 (1998).

[6] J. G. Fleming and S. Y. Lin, *Opt. Lett.* **24**, 49-51 (1999).

[7] S. Noda, K. Tomoda, N. Yamamoto, and A. Chutinan, *Science* **289**, 604-606 (2000).

[8] I. I. Tarhan and G. H. Watson, *Phys. Rev. Lett.* **76**, 315-318 (1996).

[9] W. L. Vos, R. Sprik, A. van Blaaderen, A. Imhof, A. Lagendijk, and G. H. Wegdam, *Phys. Rev. B* **53**, 16231-16235 (1996).

[10] Steven G. Johnson, John D. Joannopoulos, *Photonic Crystals: The Road from Theory to Practice*, Kluwer Academic Publishers, 14-33

[11] A. Moroz and C. Sommers, *J. Phys. Cond. Matter* **11**, 997-1008 (1999).

[12] M. S. Thijssen, R. Sprik, J. Wijnhoven, M. Megens, T. Narayanan, A. Lagendijk, and W. L. Vos, *Phys. Rev. Lett.* **83**, 2730-2733 (1999).

[13] Y. A. Vlasov, M. Deutsch, and D. J. Norris, *Appl. Phys. Lett.* **76**, 1627-1629 (2000).

[14] J. F. Bertone, P. Jiang, K. S. Hwang, D. M. Mittleman, and V. L. Colvin, *Phys. Rev. Lett.* **83**, 300-303 (1999).

[15] K. P. Velikov, A. Moroz, and A. van Blaaderen, *Appl. Phys. Lett.* **80**, 49-51 (2002).

[16] K. M. Ho, C. T. Chan, C. M. Soukoulis, R. Biswas, and M. Sigalas, *Solid State Commun.* **89**, 413-416 (1994).

[17] E. Ozbay, A. Abeyta, G. Tuttle, M. Tringides, R. Biswas, C. T. Chan, C. M. Soukoulis, and K. M. Ho, *Phys. Rev. B* **50**, 1945-1948 (1994).

[18] C. C. Cheng and A. Scherer, *J. Vac. Sci. Technol. B* **13**, 2696-2700 (1995).

[19] C. C. Cheng, A. Scherer, V. Arbet-Engels, and E. Yablonovitch, *J. Vac. Sci. Technol. B* **14**, 4110-4114 (1996).

[20] A. Birner, R. B. Wehrspohn, U. M. Gosele, and K. Busch, *Adv. Mater.* **13**, 377-388 (2001).

[21] J. Schilling, F. Muller, S. Matthias, R. B. Wehrspohn, U. Gosele, and K. Busch, *Appl. Phys. Lett.* **78**, 1180-1182 (2001).

[22] S. Shoji and S. Kawata, *Appl. Phys. Lett.* **76**, 2668-2670 (2000).

[23] M. Campbell, D. N. Sharp, M. T. Harrison, R. G. Denning, and A. J. Turberfield, *Nature* **404**, 53-56 (2000).

[24] Y. Monovoukas and A. P. Gast, *J. Colloid Interface Sci.* **128**, 533-548 (1989).

[25] P. N. Pusey, W. van Megen, P. Bartlett, B. J. Ackerson, J. G. Rarity, and S. M. Underwood, *Phys. Rev. Lett.* **63**, 2753-2756 (1989).

[26] N. A. M. Verhaegh, J. S. van Duijneveldt, A. van Blaaderen, and H. N. W. Lekkerkerker, *J. Chem. Phys.* **102**, 1416-1421 (1995).

[27] H. S. Sozuer, J. W. Haus, and R. Inguva, *Phys. Rev. B* **45**, 13962-13972 (1992).

[28] K. M. Ho, C. T. Chan, and C. M. Soukoulis, *Phys. Rev. Lett.* **65**, 3152-3155 (1990).

[29] R. Biswas, M. M. Sigalas, G. Subramania, and K. M. Ho, *Phys. Rev. B* **57**, 3701-3705 (1998).

[30] R. Biswas, M. M. Sigalas, G. Subramania, C. M. Soukoulis, and K. M. Ho, *Phys. Rev. B* **61**, 4549-4553 (2000).

[31] A. Imhof and D. J. Pine, *Nature* **389**, 948-951 (1997).

[32] A. Imhof and D. J. Pine, *Adv. Mater.* **10**, 697-700 (1998).

[33] O. D. Velev, T. A. Jede, R. F. Lobo, and A. M. Lenhoff, *Nature* **389**, 447-448 (1997).

[34] O. D. Velev, T. A. Jede, R. F. Lobo, and A. M. Lenhoff, *Chem. Mater.* **10**, 3597-3602 (1998).

[35] B. T. Holland, C. F. Blanford, and A. Stein, *Science* **281**, 538-540 (1998).

[36] B. T. Holland, C. F. Blanford, T. Do, and A. Stein, *Chem. Mater.* **11**, 795-805 (1999).

[37] J. E. G. J. Wijnhoven and W. L. Vos, *Science* **281**, 802-804 (1998).

[38] A. Imhof and D. J. Pine, *Recent Advances in Catalytic Materials*, edited by N. M. Rodriguez, S. L. Soled and J. Hrbek (Materials Research Society, Boston, 1997), Vol. 497, p. 167-172.

[39] M. Antonietti, B. Berton, C. Goeltner, and H. P. Hentze, *Adv. Mater.* **10**, 154-159 (1998).

[40] J. S. Yin and Z. L. Wang, *Adv. Mater.* **11**, 469-472 (1999).

[41] A. Richel, N. P. Johnson, and D. W. McComb, *Appl. Phys. Lett.* **76**, 1816-1818 (2000).

[42] J. Wijnhoven, L. Bechger, and W. L. Vos, *Chem. Mater.* **13**, 4486-4499 (2001).

[43] M. Muller, R. Zentel, T. Maka, S. G. Romanov, and C. M. Sotomayor Torres, *Adv. Mater.* **12**, 1499-1503 (2000).

[44] S. A. Johnson, P. J. Ollivier, and T. E. Mallouk, *Science* **283**, 963-965 (1999).

[45] A. A. Zakhidov, R. H. Baughman, Z. Iqbal, C. Cui, I. Khayrullin, S. O. Dantas, J. Marti, and V. G. Ralchenko, *Science* **282**, 897-901 (1998).

[46] Y. A. Vlasov, N. Yao, and D. J. Norris, *Adv. Mater.* **11**, 165-169 (1999).

[47] P. Jiang, K. S. Hwang, D. M. Mittleman, J. F. Bertone, and V. L. Colvin, *J. Am. Chem. Soc.* **121**, 11630-11637 (1999).

[48] A. Blanco, E. Chomski, S. Grabtchak, M. Ibisate, S. John, S. W. Leonard, C. López, F. Meseguer, H. Míguez, J. P. Mondía, G. A. Ozin, O. Toader, H. M. van Driel, *Nature* **405**, 437-440 (2000).

[49] G. Subramanian, V. N. Manoharan, J. D. Thorne, and D. J. Pine, *Adv. Mater.* **11**, 1261-1265 (1999).

[50] G. Subramania, K. Constant, R. Biswas, M. M. Sigalas, and K. M. Ho, *Appl. Phys. Lett.* **74**, 3933-3935 (1999).

[51] G. Subramania, R. Biswas, K. Constant, M. M. Sigalas, and K. M. Ho, *Phys. Rev. B* **63**, 235111 (2001).

[52] Q. B. Meng, Z. Z. Gu, O. Sato, and A. Fujishima, *Appl. Phys. Lett.* **77**, 4313-4315 (2000).

[53] O. D. Velev, P. M. Tessier, A. M. Lenhoff, and E. W. Kaler, *Nature* **401**, 548-548 (1999).

[54] P. Tessier, O. D. Velev, A. T. Kalambur, A. M. Lenhoff, J. F. Rabolt, and E. W. Kaler, *Adv. Mater.* **13**, 396-400 (2001).

[55] S. H. Park and Y. Xia, *Chem. Mater.* **10**, 1745-1747 (1998).

[56] M. Deutsch, Y. A. Vlasov, and D. J. Norris, *Adv. Mater.* **12**, 1176-1180 (2000).

[57] H. Miguez, F. Meseguer, C. Lopez-Tejeira, and J. Sanchez-Dehesa, *Adv. Mater.* **13**,

393-396 (2001).

[58] H. W. Yan, C. F. Blanford, B. T. Holland, W. H. Smyrl, and A. Stein, *Chem. Mater.* **12**, 1134-1141 (2000).

[59] N. Eradat, J. D. Huang, Z. V. Vardeny, A. A. Zakhidov, I. Khayrullin, I. Udod, and R. H. Baughman, *Synthetic Metals* **116**, 501-504 (2001).

[60] H. Miguez, E. Chomski, F. Garcia-Santamaria, M. Ibisate, S. John, C. Lopez, F. Meseguer, J. P. Mondia, G. A. Ozin, O. Toader, and H. M. van Driel, *Adv. Mater.* **13**, 1634-1637 (2001).

[61] P. Jiang, J. F. Bertone, K. S. Hwang, and V. L. Colvin, *Chem. Mater.* **11**, 2132-2140 (1999).

[62] M. E. Turner, T. J. Trentler, and V. L. Colvin, *Adv. Mater.* **13**, 180-183 (2001).

[63] S. H. Park, D. Qin, and Y. Xia, *Adv. Mater.* **10**, 1028-1032 (1998).

[64] S. H. Park and Y. Xia, *Langmuir* **15**, 266-273 (1999).

[65] B. Gates, D. Qin, and Y. Xia, *Adv. Mater.* **11**, 466-469 (1999).

[66] B. T. Mayers, B. Gates, and Y. Xia, *Adv. Mater.* **12**, 1629-1632 (2000).

[67] R. M. Amos, J. G. Rarity, P. R. Tapster, T. J. Shepherd, and S. C. Kitson, *Phys. Rev. E* **61**, 2929-2935 (2000).

[68] M. Trau, D. A. Saville, and I. A. Aksay, *Science* **272**, 706-709 (1996).

[69] M. Holgado, *et al*., *Langmuir* **15**, 4701-4704 (1999).

[70] R. C. Hayward, D. A. Saville, and I. A. Aksay, *Nature* **404**, 56-59 (2000).

[71] A. L. Rogach, N. A. Kotov, D. S. Koktysh, J. W. Ostrander, and G. A. Ragoisha,

Chem. Mater. **12**, 2721-2726 (2000).

[72] A. van Blaaderen, R. Ruel, and P. Wiltzius, *Nature* **385**, 321-324 (1997).

[73] A. van Blaaderen and P. Wiltzius, *Adv. Mater.* **9**, 833 (1997).

[74] U. Dassanayake, S. Fraden, and A. van Blaaderen, *J. Chem. Phys.* **112**, 3851-3858 (2000).

Chapter 2 Crystalline Arrays of Colloidal Spheres as Three-Dimensional Photonic Crystals

2.1 Introduction

Colloids are structures comprising small particles suspended in a liquid or a gas. Small refers to sizes between nanometers and micrometers, larger than atoms or molecules but far too small to be visible to the naked eye. Monodisperse colloidal particles can spontaneously organize into three dimensional periodic crystals. Their lattice periodicity can be easily adjusted from the nanometer to the micrometer range by varying the sizes of the particles. Their self-assembly properties make spherical colloidal particles suitable for fabricating photonic crystals.

In recent years, opal-type colloidal crystals, crystalline arrays of monodispersed spherical colloidal with closed packed structure, have been the focus of much attention with respect to applications in photonic crystals engineering: reflecting dielectric, resonant cavity, waveguide, and optical device.[2-5] Crystalline arrays of colloidal spheres, so-callled colloidal crystals or opals, and their inverse structure seem to be the most likely candidates for the photonic bandgap material.[2-5] Patterned opal or inverse opal structure were recently fabricated on silicon wafers, glass plates or other flat substrates, and inverse opals as photonic crystals with a complete bandgap were demonstrated.[6-9] Although colloidal crystals are not expected to exhibit

a full bandgap due to the relatively low dielectric contrast that can be achieved for these materials, they offer a simple and easily prepared model system to experimentally probe the photonic band diagrams of certain type of three-dimensional periodic structure.[10]

Colloidal crystals assembled from highly charged polystyrene beads or silica spheres have been known for a long time to produce Bragg diffraction of light in the optical region.[11] Spry and Kosan and Asher and co-workers noticed that the position, width, and attenuation of the Bragg diffraction peak could be described by the dynamic scattering theory that was originally put forward by Zachariasen for X-ray diffraction.[12] These highly ordered systems were recently, studied in more detail as photonic crystals by Vos et al.,[13] Watson and co-workers,[14] and several other groups. Vos et al. also concluded that the dynamic scattering theory had to be modified to take into account the excluded volume effect.[15] Lopez and co-workers,[16] Vlasov and co-workers,[17] Zhang and co-workers,[18] and Colvin and co-workers[19] have extensively investigated the photonic properties of artificial opals fabricated from monodispersed silica colloids. In some cases, the void spaces among the colloidal spheres could be infiltrated with a variety of other materials to change the dielectric contrast. Colvin and coworkers also measured the dependence of stop band attenuation on the number of layers along the [111] direction.[19]

A large colloidal crystal with a flat and uniform surface is anticipated for applications

in photonic engineering. Several methods were proposed for crystallizing spherical colloids into three dimensionally periodic lattices using sedimentation, centrifugation, electrophoresis deposition, filtration, vertical deposition, shear induction, cell packing, and liquid-air interface.[9] However, some bottlenecks exist, for example, defects, disorders and cracks formed invariably in opals and inverse opals. In our project, we modified sedimentation and vertical deposition methods to fabricate colloidal crystals with less defects, disorders and cracks. We also studied their photonic bandgap properties. The position of the stop band can be changed to cover the whole spectral region from UV to near-IR by choosing PS beads or silica spheres with different diameters. All of these studies are consistent with the computational results: that is, there only exists a pseudo bandgap for any fcc lattice self-assembled from monodispersed colloidal spheres.

2.2 Fabrication of Colloidal Crystals

2.2.1 Fabrication of Colloidal Crystals by Sedimentation

Sedimentation is the natural way to obtain solid opals. This method produces thick opals and can be altered in different ways depending on the goal pursued. In this procedure a solid is left to settle, a process that takes between days and months depending on the size of the spheres, at the end of which a sediment is obtained.[20] Figure 2.1 depicts the general procedure. The sedimentation occurs driven by gravity, and a clear sedimenting front can be seen separating clear water and colloid. The supernatant liquid is removed and the sediment dried. At this stage, the spheres are

not in actual contact but kept together by water necks. The water in the opal is about 10 wt.-% overall. The thermal treatment at 200^0C makes the sample water-free and truly compact face centered cubic (fcc), but, at the same time, mechanically very weak and unmanageable. Additionally, drying in these conditions invariably involves a crack formation process. Drying involves a contraction that does not occur in the supporting substrate, which can only be accommodated by the creation of cracks, and defects accommodate lattice mismatch in epitaxially grown materials. The final result is a compact of spheres arranged according to fcc lattice structure, whose photonic properties scale with bead diameter revealing their origin. [1, 21]

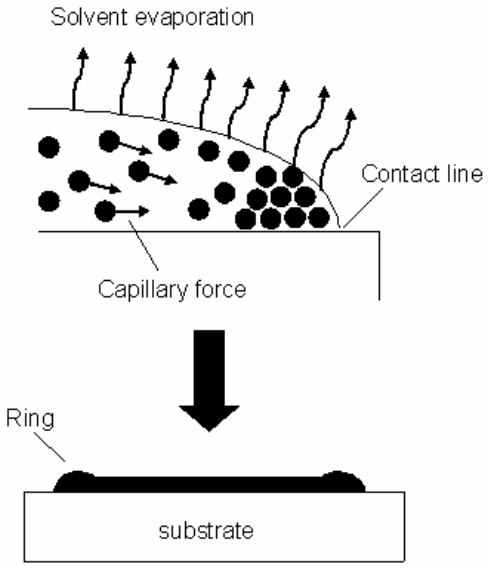

Figure 2.1. Schematic illustration of sedimentation

When beads are too large or too small (and so is their deposition velocity) bad quality or no sedimentation is achieved in a reasonable time.

Sedimentation is one of the most simple and convenient method of forming a

colloidal crystal (an opal film), but it is difficult to form a uniform and flat opal film on a flat substrate. For a coated suspension on a hydrophobic substrate, opal film will shrink during the evaporation due to the moving contact line. If a hydrophilic substrate is used, the colloidal particles accumulate at the edge of the droplet due to the pinning contact line. As a result, a ring-shape opal is formed along the contact line at the edge of the substrate. By the way, this kind of ring formation is a well-known phenomenon and is commonly observed on flat surfaces of solid substrate. Recently, this phenomenon was explained on the basis that the capillary flow causes ring stains from dried liquid drops. Deegan et al. suggested that the rate of evaporation at the edge (contact line) is greater than that at the center in a liquid suspension film.[22-24] To compensate water, the capillary flow occurs from the center to the edge; colloidal particles in the suspension are conveyed with the flow of water during crystallization. Reducing capillary flow in a colloidal suspension can depress formation of the ring as the result of dried drop suspension.[9]

In our experiments, colloidal crystals of polystyrene beads with diameter of 300nm and silica spheres with diameter of 330nm and 0.97μm were fabricated using sedimentation method. The substrates used are silicon wafers, glass and quartz plates.

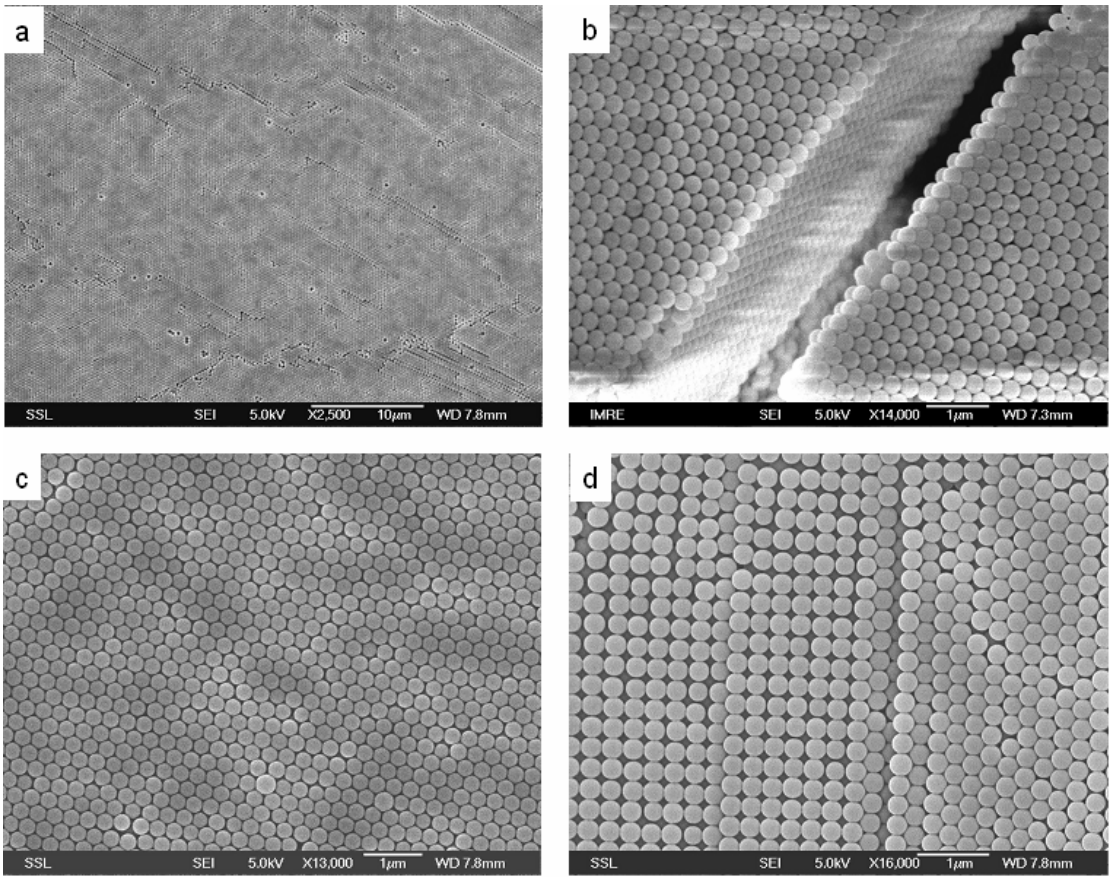

Figure 2.2. SEM images of a colloidal crystal of 300nm polystyrene beads: a) view in a large area; b) oblique view along a crack; c) view in large magnification; d) square array observed in the colloidal crystal.

Figure 2.2a shows a top view of a relative large portion of the colloidal crystal. The colloidal crystals were well ordered, but disorder and defects can also be found. The disorder and defects were generated during the crystallization, which is mainly due to the deviation of the diameter of some polystyrene beads. Figure 2.2b shows an oblique view of the crystal along a crack and indicates that the polystyrene beads formed a cubic-close-packed (ccp) structure that extends all layers along the direction perpendicular to the surfaces of the substrate. The ccp structure can also be described as a face-centered cubic (fcc) lattice with the (111) face parallel to the surfaces of the substrate. The crack in the crystal was created as a result of the volume shrinkage of wet colloidal crystal during the drying process. Figure 2.2c and d show a top view of

the crystal in large magnification. The (111) face (hexagonal array) can be found in most area of the surface, but the (100) face (square array) can also be observed. The proportion of the square array over the entire surface is about 20%, which is much lower than that of the hexagonal array.

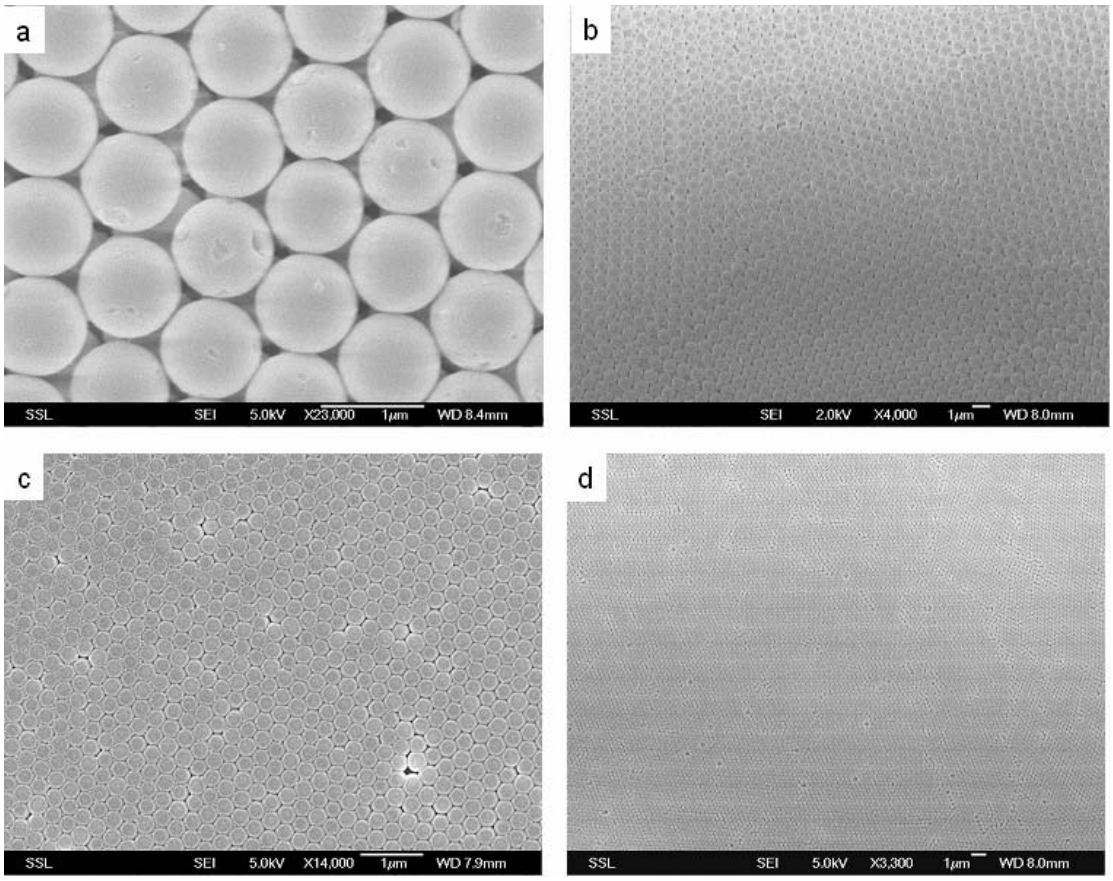

Figure 2.3. a, b) SEM images of colloidal crystal of 0.97μm silica spheres in large and small magnification; c, d) SEM images of colloidal crystal of 0.33μm silica spheres in large and small magnification.

Figure 2.3a, b, c and d show SEM images of the colloidal crystal of silica spheres with diameter of 0.97μm and 0.33μm, respectively. The crystals also had a structure of fcc lattice with (111) plane parallel to the surfaces of substrates.

2.2.2 Fabrication of Colloidal Crystals by Vertical Deposition

The set up of the vertical deposition is simple and only requires a vial containing a colloid (typically about 1 vol.-%), where a flat substrate is inserted vertically. Figure 2.4 illustrates the general procedure of vertical deposition. A meniscus is formed that draws particles to its vicinity by capillarity. Evaporation sweeps the meniscus along the substrate vertically, feeding particles to the growth of front. Colloid concentration and sphere diameter determine the thickness of the layer deposited. Successive growth process can lead to the assembly of multilayers that can be constituted of similar or different particles.[1] Under the proper conditions, evaporation of the solvent leads to the deposition of an ordered three-dimensional packing of spheres with more or less uniform thickness on the substrate, starting form a position below the initial level of the contact line at the top of the meniscus. Once the opal film is dried, the colloidal spheres adhere well enough to the adjacent ones, and to the substrate that the film can be easily handled without detaching or disintegrating.

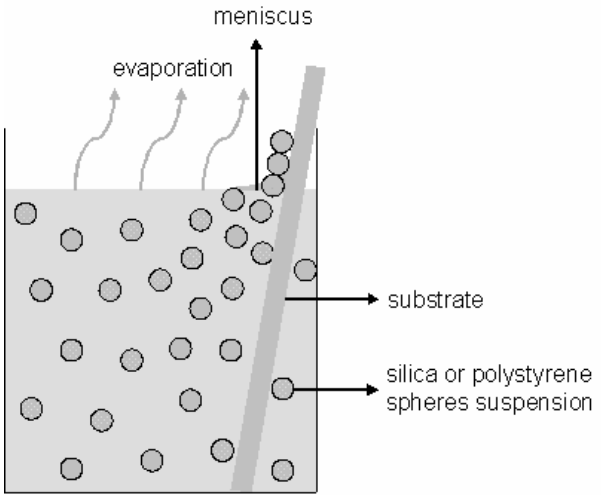

Figure 2.4. Schematic illustration of vertical deposition

Although the evaporation rate can be easily controlled through the vapor pressure in

the surrounding atmosphere, controlling the sedimentation rate is not so easy as it is largely determined by sphere size. When the spheres are smaller than 400nm, successful conditions are relatively easy to achieve.[25] The solvent (typically water) is simply evaporated slowly form the suspension at room temperature. However, for larger spheres, this simple approach is unsuccessful. The spheres sediment quickly and are not deposited. This problem was overcome by choosing a more volatile solvent (ethanol) and application of a temperature gradient to the vial.[26, 27] Now this method can produce high-quality opal films with uniform structure over a relatively large area (larger than 1 cm^2).[28-33]

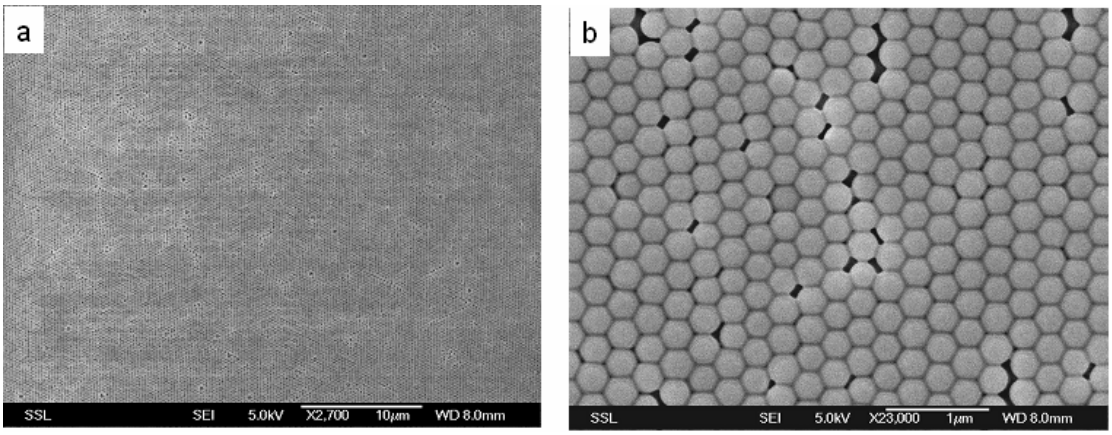

Figure 2.5. SEM images of a colloidal crystal of 0.33μm silica spheres using vertical deposition: a) view in small magnification; b) view in large magnification.

Figure 2.5 shows SEM images of a colloidal crystal of 0.33μm silica spheres obtained by using vertical deposition method. The structure of the crystal is similar to that of colloidal crystals formed using sedimentation method, but the quality of the crystal is much better and no discernible crack can be observed in a quite large area (large than 200 μm× 200 μm). Further experiments showed that the number of layers of colloidal

crystals was increased with increasing the concentration of suspension within the limitation of 10% by weight.

2.3 Optical Characterization of Colloidal Crystals

Optical reflection and transmission measurement were obtained at normal incidence to the substrate using UV-Vis spectrometer.

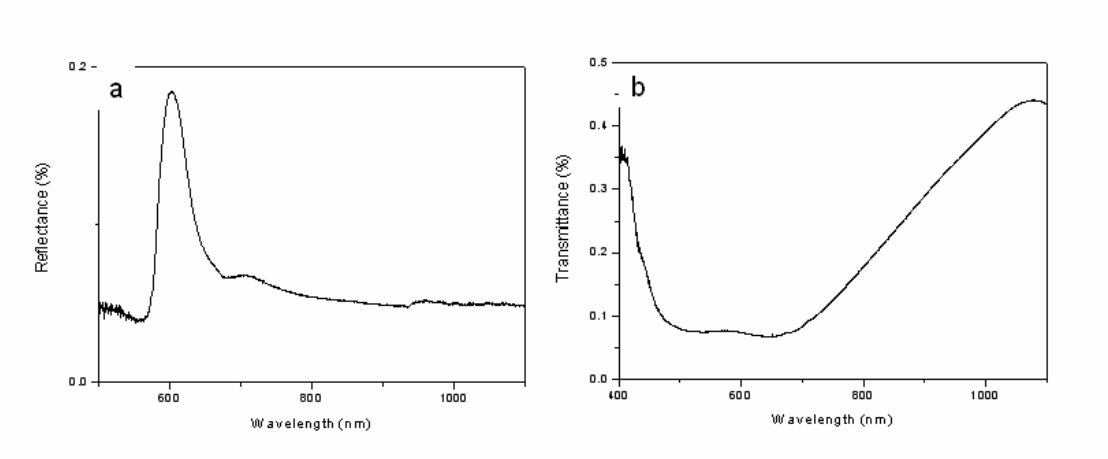

Figure 2.6. UV-Vis reflectance and transmission spectra of a colloidal crystal assembled from 300nm polystyrene beads with the incident light normal to the substrate.

Figure 2.6 shows the reflectance and transmission spectra of the colloidal crystal assembled from 300 nm polystyrene microspheres prepared by sedimentation. The peak position and dip position, which correspond to the first Bragg diffraction (the stop band), are located at 604nm. The relatively low reflectance observed in the experimental measurements was probably caused by the diffusive scattering of cracks formed during sample drying, since the size of the optical probe we used was several millimeters in diameter. This scattering effect is also expected to increase the width of the diffraction peak (the stop band). The transmission spectrum shows a wider and

shallower stop band. Recent studies reveal that the defects in colloidal crystals strongly affect their optical properties.[34] The presence of defects results in the appearance of strongly localized photonic bandtail states, and thus enhances the transmission in the gap, so the stop band will become shallower with the presence of disorder. The transmission in the gap increases with the increase of disorder. On the other hand, the presence of defects leads to exponential decay of light with thickness not only within the former gap of the periodic structure, but also in the former passbands, thus broadening the gap and decreasing the transmission in the passbands.

The 3D crystalline array of colloidal spheres diffracts light according to the Bragg equation:[35]

$$m\lambda_{\min} = 2d_{hkl}(n^2 - \sin^2\theta)^{1/2} \tag{2.1}$$

where *m* is the order of diffraction; $\lambda_{\min}$ is the position of diffraction peak observed on the reflection or transmission spectra (or the stop band); d_{hkl} is the spacing between (*hkl*) planes; θ is the angle between the incident light and the normal to the diffraction planes (at normal incidence, $\theta = 0$); and *n* is the mean refractive index of this crystalline lattice. In this case, d_{111} becomes $(2/3)^{1/2} D$, where D is the diameter of PS beads. As a good approximation, *n* can be calculated using the following formula:

$$n = n_p f + n_m(1 - f) \tag{2.2}$$

where n_p is the refractive index of colloidal particles; *f* is the volume fraction occupied by the particles; and n_m represents the refractive index of air in the crystals.

In this case, n_p = 1.6, n_m = 1, and the volume fraction was f = 0.74 for samples made of PS spheres. As a result, the mean refractive index of the PS colloidal crystals should be 1.444. The first order diffraction peak at 604nm corresponding to a lattice spacing of 245nm between the (111) planes perpendicular to the incident light.

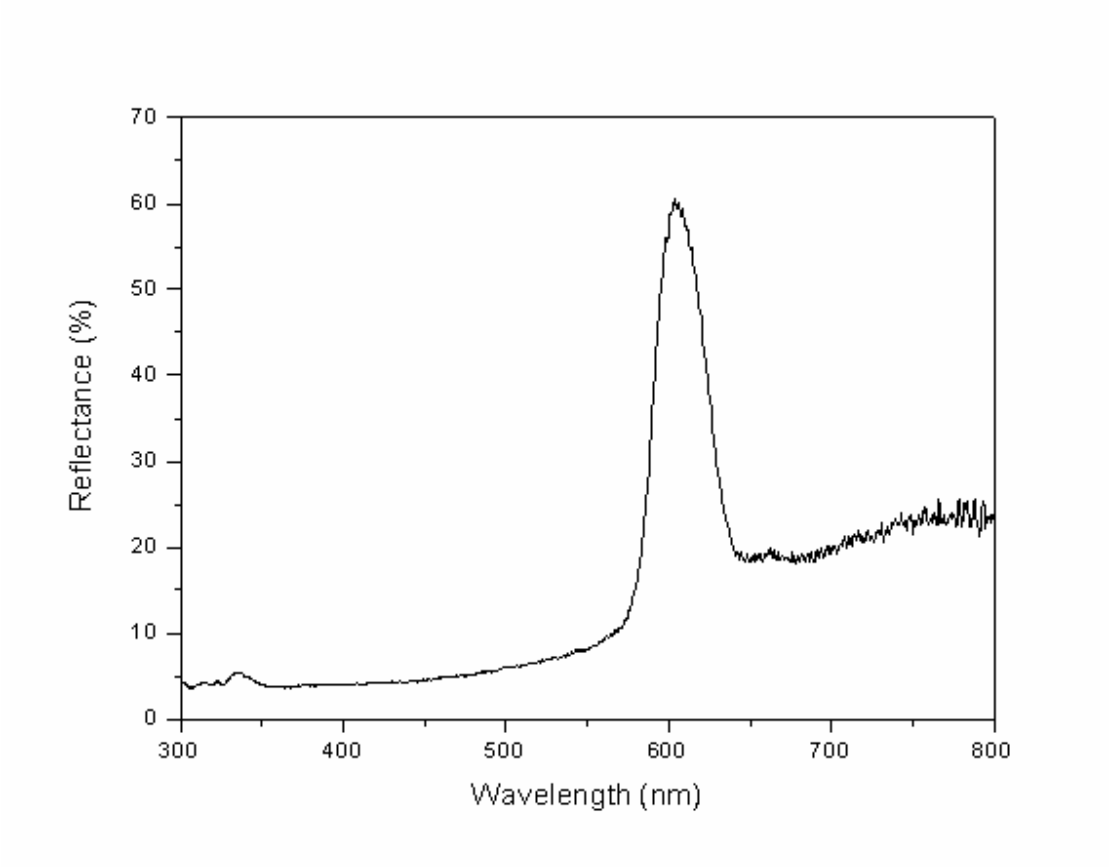

Figure 2.7. UV-Vis reflectance spectrum of a colloidal crystal of 0.33μm silica spheres with the incident light normal to the substrate.

Figure 2.7 shows the reflectance spectrum of a colloidal crystal of 0.33μm silica spheres prepared by vertical deposition. In this case, n_p = 1.45, n_m = 1, and the volume fraction was f = 0.74 for samples made of silica spheres. As a result, the mean refractive index of the silica colloidal crystals should be 1.333. The stop band position displayed as peak position is located at 603nm, which corresponds to a lattice spacing

of 269nm between the (111) planes perpendicular to the incident light.

2.4 Conclusions

In summary, colloidal crystals were fabricated from polystyrene and silica colloidal particles by sedimentation and vertical deposition. The crystals with structure of face centered cubic (fcc) lattice were resulted from evaporation-induced interfacial self-assembly crystallization. Through optimizing the fabrication conditions in terms of crystallizing temperature and the concentration of the particles, the defects, disorders and cracks in the colloidal crystals are greatly reduced and the typical size of a single crystalline domain is larger than 200μm. Their reflectance spectra measured with UV-Vis spectrometer show that they possess photonic stop bandgaps.

References

[1] Cefe Lopez, *Adv. Mater.* **15**, 1679-1704 (2003).

[2] O.D. Velev, A.M. Lenhoff, Curr. Opin. *Colloid Interface Sci.* **56**, 5 (2000).

[3] D.G. Grier (Ed.), *From Dynamics to Devices: Directed Self-Assembly of Colloidal Materials (special issue), MRS Bull.* **23**, 21 (1998).

[4] Y. Xia, B. Gates, Y. Yin, Y. Lu, *Adv. Mater.* **12**, 693 (2000).

[5] A.D. Dinsmore, J.C. Crocker, A.G. Yodh, Curr. Opin. *Colloid Interface* **3**, 5 (1998).

[6] Y.A. Vlasov, X.Z. Bo, J.C. Sturm, D.J. Norris, *Nature* **414**, 289 (2001).

[7] Y. Yin, Y. Liu, Y. Xia, *J. Am. Chem. Soc.* **23,** 771 (2001).

[8] G.A. Ozin, S.M. Yang, *Adv. Funct. Mater.* **11,** 95 (2001).

[9] Hiroshi Fudouzi, *Journal of Colloidal and Interface Science* **275,** 277-283 (2004).

[10] Younan, Xia, Byron Gates, Yadong, Yin, and Yu Lu, *Adv. Mater.* **12**, 693-713 (2000).

[11] a) P. L. Flaugh, S. E. O'Donnell, S. A. Asher, *Appl. Spectrosc.* **38**, 847 (1984). b) J. W. Goodwin, R. H. Ottewill, A. Parentich, *J. Phys. Chem.* **84**, 1580 (1980).

[12] P. A. Rundquist, P. Photinos, S. Jagannathan, S. A. Asher, *J. Chem. Phys*. **91**, 4932 (1989).

[13] W. L. Vos, R. Sprik, A. van Blaaderen, A. Imhof, A. Lagendijk, G. H. Wegdam, *Phys. Rev. B* **53**, 16231 (1996).

[14] I. I. Tarhan, G. H.Watson, *Phys. Rev. Lett.* **76**, 315 (1996).

[15] W. L. Vos, M. Megens, C. M. van Kats, P. Bosecke, *J. Phys.: Condens. Matter* **8**, 9503 (1996).

[16] a) R. Mayoral, J. Requena, J. S. Moya, C. Lopez, A. Cintas, H. Miguez, F. Meseguer, L. Vazquez, M. Holgado, A. Blanco, *Adv. Mater.* **9**, 257 (1997). b) H. Miguez, C. Lopez, F. Mesequer, A. Blanco, L. Vazquez, R. Mayoral, M. Ocana, V. Fornes, A. Mifsud, *Appl. Phys. Lett.* **71**, 1148 (1997). c) C. Lopez, L. Vazquez, F. Meseguer, R. Mayoral, M. Ocana, H. Miguez, *Superlattices Microstruct.* **22**, 399 (1997).

[17] a) V. N. Astratov, Y. A. Vlasov, O. Z. Karimov, A. A. Kaplyanskii, Y. G. Musikhin, N. A. Bert, V. N. Bogomolov, A. V. Prokofiev, *Phys. Lett. A* **222**, 349 (1996). b) Y. A. Vlasov, V. N. Astratov, O. Z. Karimov, A. A. Kaplyanskii, V. N.

Bogomolov, A. V. Prokofiev, *Phys. Rev. B* **55**, R13 357 (1997).

[18] D. Mei, H. Liu, B. Cheng, Z. Li, D. Zhang, *Phys. Rev. B* **58**, 35 (1998).

[19] J. F. Bertone, P. Jiang, K. S. Hwang, D. M. Mittleman, V. L. Colvin, *Phys. Rev. Lett.* **83**, 300 (1999).

[20] R. Mayoral, J. Requena, J. S. Moya, C. Lopez, A. Cintas, H. Miguez, F.Meseguer, L. Vazquez, M. Holgado, A. Blanco, *Adv. Mater*. **9**, 257 (1997).

[21] H. Miguez, F. Meseguer, C. Lopez, A. Mifsud, J. S. Moya, L. Vazquez, *Langmuir* **13**, 6009 (1997).

[22] R.D. Deegan, O. Bakajin, T.F. Dupont, G. Huber, S.R. Nagel, T.A. Witten, *Nature* **389**, 827 (1997).

[23] R.D. Deegan, *Phys. Rev. E* **61**, 475 (2000).

[24] R.D. Deegan, O. Bakajin, T.F. Dupont, G. Huber, S.R. Nagel, T.A. Witten, *Phys. Rev. E* **62**, 756 (2000).

[25] P. Jiang, J. F. Bertone, K. S. Hwang, V. L. Colvin, *Chem. Mater.* **11**, 2132 (1999).

[26] D. J. Norris, Yu. A. Vlasov, *Photonic Crystals and Light Localization* (Ed: C. M. Soukoulis), Kluwer, Dordrecht, The Netherlands, p. 229 (2001).

[27] Yu. A. Vlasov, X. Z. Bo, J. C. Sturm, D. J. Norris, *Nature* **414**, 289 (2001).

[28] L. M. Goldenberg, J. Wagner, J. Stumpe, B. R. Paulke, E. Gornitz, *Langmuir* **18**, 3319 (2002).

[29] S. H. Im, M. H. Kim, O. O. Park, *Chem. Mater.* **15**, 1797 (2003).

[30] L. Cademartiri, A. Sutti, G. Calestani, C. Dionigi, P. Nozar, A. Mighori, *Langmuir* **19**, 7944 (2003).

[31] H. Cong, W. X. Cao, *Langmuir* **19**, 8177 (2003).

[32] S. Wong, V. Kitaev, G. A. Ozin, *J. Am. Chem. Soc.* **125**, 15 589 (2003).

[33] M. A. McLachlan, N. P. Johnson, R. M. D. L. Rue, D. W. McComb, *J. Mater. Chem.* **14**, 144 (2004).

[34] Yong-Hong Ye, Francois LeBlanc, Alain Hache, and Vo-Van Truong, *Appl. Phys. Lett.* 78, 52-54 (2000).

[35] (a) A. Richel, N.P. Johnson, D.W. McComb, *Appl. Phys. Lett.* **76**, 1816 (2000).

(b) S.G. Romanov, T. Maka, C.M.S. Torres, M. Muller, R. Zentel, D. Cassagne, J.Manzanares-Martinez, C. Jouanin, *Phys. Rev. E* **63**, 056603 (2000).

Chapter 3 Effects of Surfactant on Structure of Colloidal Crystals

3.1 Introduction

3.1.1 Research Background

Monodispersed spherical colloidal particles can spontaneously form three-dimensionally periodic lattices (or colloidal crystals) as a direct consequence of various types of thermodynamic driving forces.[1] These crystalline assemblies of mesoscale particles have been recognized as a unique model system to explore fundamental phenomena of condensed matter physics that include, for example, phase transition,[2] nucleation,[3] and diffusion.[4] More recently, colloidal crystals have become a subject of intensive research, because of their photonic applications as optical filters,[5] switches,[6] sensors,[7] and waveguiding structures.[8]

Colloidal crystals can be easily fabricated through self-assembly techniques from microspheres made of SiO2 or polymers, adopting face-centered-cubic (fcc) lattices.[9–12] Evaporation-induced self-assembly, patterned substrates, and physical confinement have been used to direct the colloidal crystal growth. The (111) or (100) surface of the fcc crystal is typically parallel to the surface of the substrate.[13–20] However, investigations related to the array fashion of the particles are very limited. Dushkin et al.[21, 22] studied the effect of water evaporation rate, liquid meniscus at the boundary, particle size, etc. on circular-shaped crystals formed from a thin layer of a

latex suspension. The authors mentioned that a hexagonal lattice from monodispersed colloids prevails in the formed crystal, but square lattices can be observed in the transition regions between hexagonal lattices. Also, the formation of square arrays is favorable by addition of glucose, which decreases the particle movement. Weixiao Cao et al.[23] investigated the effects of temperature and surfactant on the array fashions of the particles as well as the packing modes of the crystals. They concluded that the deposition temperature and surface tension of the latex solution play important roles in determining the structure of the formed colloidal crystals.

To further understand the array fashion of the particles and obtain colloidal crystals with high quality and desired structures, different surfactants were added into polystyrene colloids for fabricating colloidal crystals in our experiments.

3.1.2 Surfactants

Surfactant has two distinct parts in the same molecule; one that has an affinity for the solvent and the other that does not. In aqueous solutions, these two moieties are hydrophilic and hydrophobic parts respectively. The hydrophilic part is usually referred to as ‘head group’ and is either strongly polar or charged. The hydrophobic part is usually called the ‘tail’ and is most commonly a simple hydrocarbon group. If surfactant molecules are located at an air–water or oil-water interface, they are able to locate their hydrophilic head groups in the aqueous phase and allow the hydrophobic hydrocarbon chains to escape into the air or oil phase. This situation is more

energetically favorable than complete solution in either phase. The strong adsorption of such material at surfaces or interfaces in the form of an orientated monomolecular layer (or monolayer) is termed as surface activity. Surfactants are classified as anionic, cationic, zwitterionic (or amphoteric) and nonionic according to the charge carried by the head group.

It is well known that when a hydrocarbon chain is in contact with water, the network of hydrogen bonds between water molecules reconstructs itself to avoid the region occupied by the hydrocarbon. This constraint on the local structure of water decreases the entropy of the water near the hydrocarbon and results in a larger free energy for the total system. The hydrophobic effect, therefore, arises because of the self-attraction of water for itself, which tends to squeeze the hydrocarbon out and not because of repulsion between water and hydrocarbon. This leads to the tendency of the surfactant molecules to self-association or aggregation, so that the energetically unfavorable contact between the nonpolar part and water can be avoided while the polar part retains the aqueous environment. Micelle is an aggregate formed by self association of amphiphilic molecules in water, in which the hydrocarbon chains are in the middle, avoiding contact with water as much as possible, and the hydrophilic groups are at the surface. The concentration above which micelle formation becomes appreciable is termed as the critical micelle concentration or CMC. Once CMC is reached, further addition of surfactant causes the formation of aggregates or micelles. All additional surfactant aggregates into micelles and the monomer concentration

remains almost constant. Figure 3.1 shows the schematic illustration of the micelle formation in aqueous solution and the surface tension as a function of surfactant concentration. Even at very low concentrations, surfactants lower the surface tension of water quite appreciably. But at concentration above CMC, for pure surfactants, the surface tension remains constant. Since the micelles themselves are not surface-active, the surface tension remains approximately constant beyond CMC.

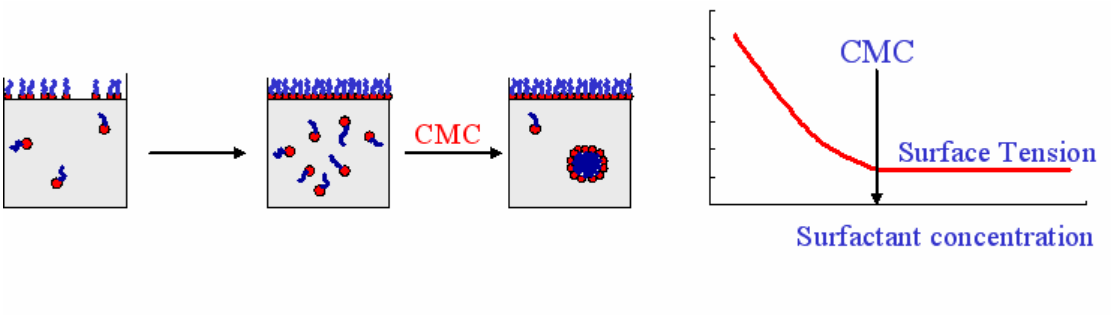

Figure 3.1. Schematic illustration of micelle formation in aqueous solution and surface tension as a function of surfactant concentration.

3.2 Preparation and Characterization of Colloidal Crystals with Surfactants

The colloidal crystals were prepared from monodispersed polystyrene colloids with addition of surfactants by sedimentation. The diameter of the polystyrene beads is 0.3μm. Four kinds of surfactants, which are dodecyl sulfate, sodium salt (SDS), glycolic acid ethoxylate lauryl ether (GAELE), hexadecyltrimethylammonium bromide (CTAB), and polyoxyethylenesorbitan monooleate (Tween 80), were used to study the effect of surfactant on the structure of colloidal crystals. SDS and GAELE are anionic surfactants; CTAB is a cationic surfactant; Tween 80 is a nonionic

surfactant. For each kind of surfactant, different concentrations were used. Table 3.1 shows their CMC and different concentrations of the surfactants in PS colloids for fabricating colloidal crystals.

Table 3.1. Surfactants with different concentrations in PS colloids for fabricating colloidal crystals

	Sample 1 (mg/ml)	Sample 2 (mg/ml)	Sample 3 (mg/ml)	Sample 4 (mg/ml)
SDS Anionic CMC=2.30mg/ml	3.07	---	---	---
GAELE Anionic CMC=0.185mg/ml	0.07	0.13	0.21	---
CTAB Cationic CMC=0.35mg/ml	0.17	0.70		---
Tween 80 Nonionic CMC=0.013mg/ml	0.00625	0.0125	0.021	0.122

A scanning electron microscope (SEM) was used to observe the structures and morphologies of the resulting colloidal crystals. Several observations were performed on a 50 μm×50 μm area, which was selected arbitrarily on the sample surfaces. Then the representative structure or morphology was determined as an image.

3.3 Results and Discussion

Figure 3.2a shows a SEM image of the colloidal crystal formed in the presence of

SDS. The concentration of SDS in PS suspension is 3.07 mg/ml, which is above its CMC. The image shows that hexagonal array prevailed in the formed crystal, but square array can also be observed. The result is similar to that reported by Dushkin and Weixiao Cao et al. for colloidal crystals from polystyrene latex.[21-23] The square array has more interspaces than the hexagonal array. The proportion of the square array over the entire surface of the colloidal crystal formed in the presence of SDS increase to about 30% as compared to that formed in the absence of SDS (about 20%). Figure 3.2b, c and d show SEM images of the colloidal crystals formed in the presence of GAELE with different concentrations. The colloidal crystals have similar morphology and structure compared to that formed in the presence of SDS. The presence of GAELE with different concentrations has not much effect on the proportion of the square array.

Figure 3.3a and b show SEM images of the colloidal crystals formed in the presence of CTAB with concentration of 0.17 mg/ml and 0.70 mg/ml, respectively. The images show that the colloidal crystals maintained fcc lattice structure, but disordered fractal aggregates appeared on the sample surfaces. Furthermore, it seems that more aggregates will appear with increasing the concentration and the particles on the top layer were not well ordered when the concentration is high enough.

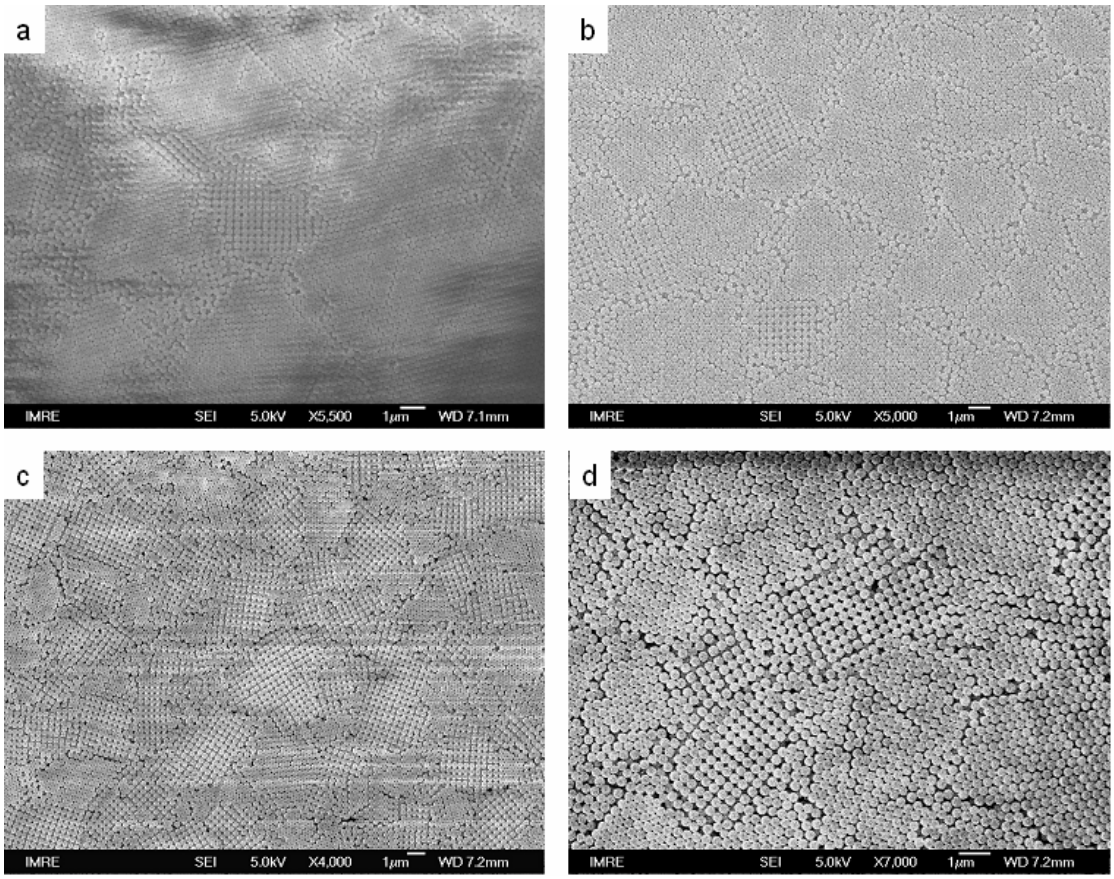

Figure 3.2. SEM images of colloidal crystals formed in the presence of surfactants a) SDS, conc. = 3.07 mg/ml; b) GAELE, conc. = 0.07 mg/ml; c) GAELE, conc. = 0.13 mg/ml; d) GAELE, conc. = 0.21 mg/ml.

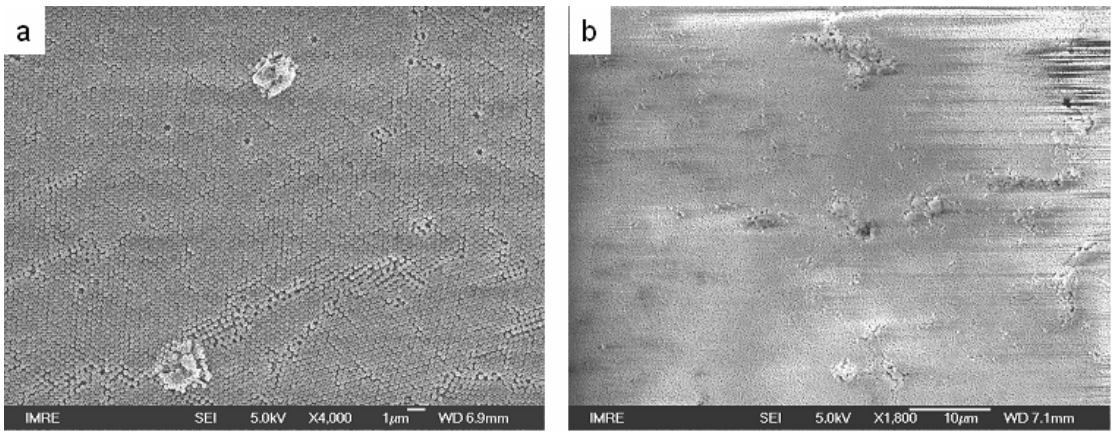

Figure 3.3. SEM images of colloidal crystals formed in the presence of CTAB. a) conc. = 0.17 mg/ml; b) conc. = 0.70 mg/ml.

Figure 3.4a, b, c and d show SEM images of the colloidal crystals formed in the presence of Tween 80 with concentration of 0.00625 mg/ml, 0.0125 mg/ml, 0.021

mg/ml and 0.122 mg/ml, respectively. When the concentration of Tween 80 was below or equal to its CMC (Figure 3.4a, b), the colloidal crystals show the similar morphology and structure to those formed in the presence of SDS and GAELE, and two different arrays can also be observed. When the concentration of Tween 80 was about two times of its CMC (Figure 3.4c), small domains of square array occupied nearly the whole surface of the sample. When the concentration was well above its CMC (Figure 3.4d), small aggregates of Tween 80 molecules appeared on each particle on the sample surface, but the PS microspheres still self-organize into to an fcc crystalline with (111) plane parallel to the substrate.

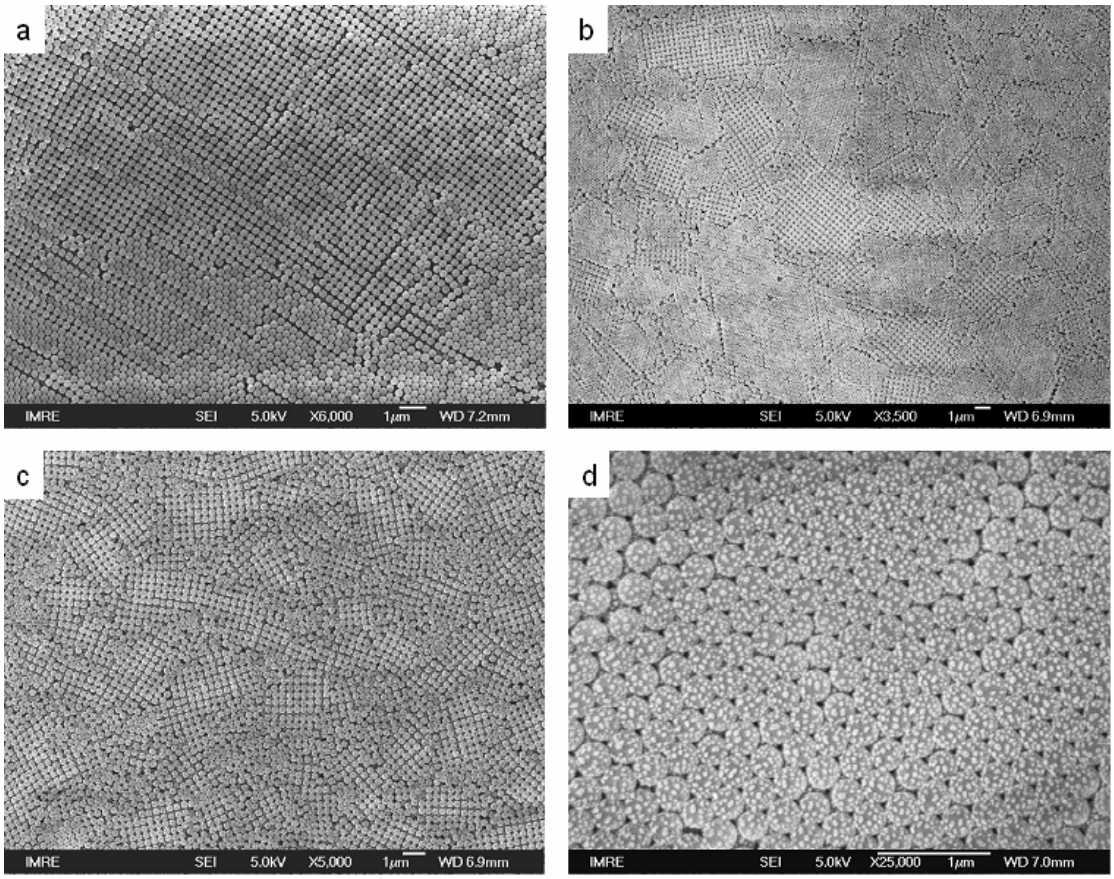

Figure 3.4. SEM images of colloidal crystals with addition of Tween 80. a) conc. = 0.00625 mg/ml; b) conc. = 0.0125 mg/ml; c) conc. = 0. 021 mg/ml; d) conc. = 0.122 mg/ml.

To explain the phenomena, a great attention must be paid to controlling the interaction energies between the particles and between the particles and their surroundings. Thermally induced self-assembly typically requires repulsive or only very weakly attractive interactions. Strong attraction usually leads to the formation of highly disordered aggregates, rather than ordered colloidal crystal structures.[24] Thus, for CTAB, when charge-stabilized colloidal particles are mixed with the opposite charged surfactant, they typically destabilize and form disordered aggregates. Because the surfactant binds electrostatically to the particles, this process makes their surfaces hydrophobic and leads to strongly attractive particles interactions. For SDS and GAELE, well ordered colloidal crystals formed because the surfactants have the same charge and do not much affect the interaction between particles so much. As for more square arrays on the surfaces, it is due to the thermal energy has been changed a little by surfactants. For Tween 80, when the concentration is below or a little above its CMC well ordered colloidal crystals still formed and more arrays appeared on the surface compared to those formed in the absence of surfactant. Because the surfactant does not have any charge and the interaction between particles will not be affected so much. When the concentration is well above its CMC, the micelles of Tween 80 molecules became large enough and aggregated, appearing on each particle when the sample dried.

3.4 Conclusions

Colloidal crystals were fabricated in the presence of different surfactants with

different concentrations by sedimentation. The surfactants are effective in modifying the orientation of colloidal crystals. The square array is favorable to form in the presence of surfactants that change the interaction between the colloidal particles. This provides an effective route for control of the orientation of colloidal crystals and may have potential applications.

References

[1] (a) *From Dynamics to Devices*: *Directed Self-Assembly of Colloidal Materials* (Grier, D. G., Ed.), a special issue of *MRS Bull.* (1998, **23**, 21). (b) Xia, Y.; Gates, B.; Yin, Y.; Lu, Y. *Adv. Mater.* **12**, 693 (2000).

[2] Murray, C. A.; Grier, D. G. *Am. Sci.* **83**, 238 (1995).

[3] Skjeltorp, A. P.; Meakin, P. *Nature* **335**, 424 (1988).

[4] Simon, R.; Palberg, T.; Leiderer, P. *J. Chem. Phys.* **99**, 3030 (1993).

[5] Weissman, J. M.; Sunkara, H. B.; Tse, A. S.; Asher, S. A. *Science* **274**, 959 (1996).

[6] Pan, G.; Kesavamoorthy, R.; Asher, S. A. *Phys. Rev. Lett.* **78**, 3860 (1997).

[7] Holtz, J. H.; Asher, S. A. *Nature* **389**, 829 (1997).

[8] Lee, W.; Pruzinsky, S. A.; Braun, P. V. *Adv. Mater.* **14**, 271 (2002).

[9] A. Blanco, E. Chomski, S. Grabtchak, M. Ibisate, S. John, S. W. Leonard, C. López, F. Meseguer, H. Míguez, J. P. Mondia, G. Ozin, O. Toader, and H. M. van Driel, *Nature* **405**, 437 (2000).

[10] Y. A. Vlasov, X. Bo, J. C. Sturm, and D. J. Norris, *Nature* **414**, 289 (2001).

[11] B. Holland, C. Blanford, and A. Stein, *Science* **281**, 538 (1998).

[12] S. Wang, V. Kitaev, and G. A. Ozin, *J. Am. Chem. Soc.* **125**, 15589 (2003).

[13] E. Kim, Y. Xia, and G. M. Whitesides, *Adv. Mater.* **8**, 245 (1996).

[14] A. Blaaderen, R. Ruel, and P. Wiltzius, *Nature* **385**, 321 (1997).

[15] S. M. Yang and G. A. Ozin, *Chem. Commun.* **24**, 2507 (2000).

[16] H. Míguez, S. M. Yang, N. Tétreault, and G. A. Ozin, *Adv. Mater.* **14**, 1805 (2002).

[17] S. M. Yang, H. Miguez, and G. Ozin, *Adv. Funct. Mater.* **12**, 425 (2002).

[18] Y. Yin, Z. Li, and Y. Xia, *Langmuir* **19**, 622 (2003).

[19] J. Zhang, A. Alsayed, K. H. Lin, S. Sanyal, F. Zhang, W. J. Pao, V. S. K. Balagurusamy, P. A. Heiney, and A. G. Yodh, *Appl. Phys. Lett.* **81**, 3176 (2002).

[20] B. Gates, Y. Lu, Z. Y. Li, and Y. Xia, *Appl. Phys. A: Mater. Sci. Process.* **76**, 509 (2003).

[21] Dushkin, C. D.; Yoshimura, H.; Nagayama, K. *Chem. Phys. Lett.* **204**, 45 (1993).

[22] Dushkin, C. D.; Lazarov, G. S.; Kotsev, S. N.; Yoshimura, H.; Nagayama, K. *Colloid Polym. Sci.* **277**, 914 (1999).

[23] Hailin Cong and Weixiao Cao, *Langmiur* **19**, 8177-8181 (2003).

[24] Laurence Ramos, T. C. Lubensky, Nily Dan, Philip Nelson, D. A. Weitz, *Science* **286**, 2325-2327 (1999).

Chapter 4 Effects of Pre-heating Treatment on Photonic Bandgap Properties of Silica Colloidal Crystals

4.1 Introduction

Photonic bandgap (PBG) crystals have attracted great attention because of their potential applications in confining and controlling electromagnetic waves in all three directions of space. [1-3] These structures consist of periodic dielectric materials, which strongly diffract light and exhibit a stop band in its reflectance and transmission spectrum. [4, 5] Recently, the three-dimensional (3D) PBG crystals formed from monodispersed particles, both organic and inorganic, have been proposed as an easy and low-cost way to fabricated 3D PBG and a suitable system to investigate the optical properties. [6-8] The photonic crystal properties can be easily tuned by the sphere diameter, covering the whole visible and NIR region of the spectrum. It has been demonstrated that the position of the stop band can be tuned by sintering the self-assembly crystals at elevated temperature. [9, 10] In this case, the position (and intensity) of the stop band could be changed in a controllable way to cover a narrow spectral region.

The particles in pristine samples of silica colloids have the ultramicroporous structure and will undergo a series of changes when they are thermally treated at elevated temperatures. The absorbed water (about 5% by weight) will be released first at around 150^0C; the silanol groups will be crosslinked via dehydration in the temperature range of 400-700^0C; and these particle will start to fuse into aggregates when the temperature is raised above

the glass transition temperature of amorphous silica (about 800^0C). [11] Thus, the size, density and refractive index of the particles may change after their heating treatment. Based on this feature of silica colloidal particles, we explored pre-heating treatment to control the photonic bandgap properties of silica colloidal crystals. In our experiments, colloidal crystals were fabricated from silica colloidal particles that were preheated at different temperatures for 2 hours prior to assembly. The results show that this is an alternative way to tune the photonic bandgap properties. In contrast to the former post-annealing method, the pre-heating method facilitates the integration of the photonic crystals with other optical or electrical components by avoiding applying high temperature that may cause damage to some heat-sensitive devices. Furthermore, the silica colloidal crystals can be used as templates to fabricate inverse opals with photonic bandgaps in specific region of the spectrum.

4.2 Experiments

Silica colloids from Bangs Laboratories were placed in small vials and sintered as dry powders at 250^0C, 350^0C, 450^0C, 550^0C and 650^0C, respectively. For each case, the heating rate is 5^0C per minute during temperature increase process and the heating duration is 2 hours when the temperatures reached the required values. The average diameter of the original silica spheres measured by field emission scanning electron microscope (SEM, JSM-6700, JEOL) was 290nm. After sintering, the particles were redispersed in deionized water by using ultrasonication (about 1.7% by volume) and cleaned glass plates with dimension of 40mm×8mm×1mm were placed nearly vertically into the vials. To assemble 3D silica colloidal crystals (opals) with high crystalline

quality over large areas, the vials and one containing original silica colloid for comparison were put in an oven and the temperature was maintained as 65^0C based on a report on the optimum crystallization temperature for fabrication of opals. [12] As the solvent evaporated, thin opals were deposited on the substrates. Optical reflectance of the samples on the glass substrates were obtained at the normal incidence to the substrates using UV-Vis spectrometer in the wavelength range of 300-800nm.

4.3 Results and Discussion

The samples were studied using a scanning electron microscopy (SEM). Figure 4.1 shows typical SEM images of silica colloidal crystals. Figure 4.1a is taken from the colloidal crystal of original silica spheres and Figure 4.1b is taken from the colloid crystal of silica spheres with pre-heating treatment at 650^0C for 2 hours. The image in Figure 4.1b indicates that the shape of each silica particle maintained spherical after heating treatment. The change of the crystal structures is not observed. Both of the crystals have the lattice of face centered cube (fcc) with the (111) plane parallel to the surfaces of substrates. Comparing the size of the untreated particles and the pre-treated particles, the pre-heated particles are shrunk.

Changes in the size of the spheres were obtained from SEM images. About 100 particles were measured for determining the size of the particles heated at different temperatures. Figure 4.2 illustrates the relationship between the sizes of spheres and pre-heating temperatures. The data show that the spheres shrink after heating treatment and the size of spheres decreases with heating temperature, T, and it levels off at about $T \geq 350^0$C.

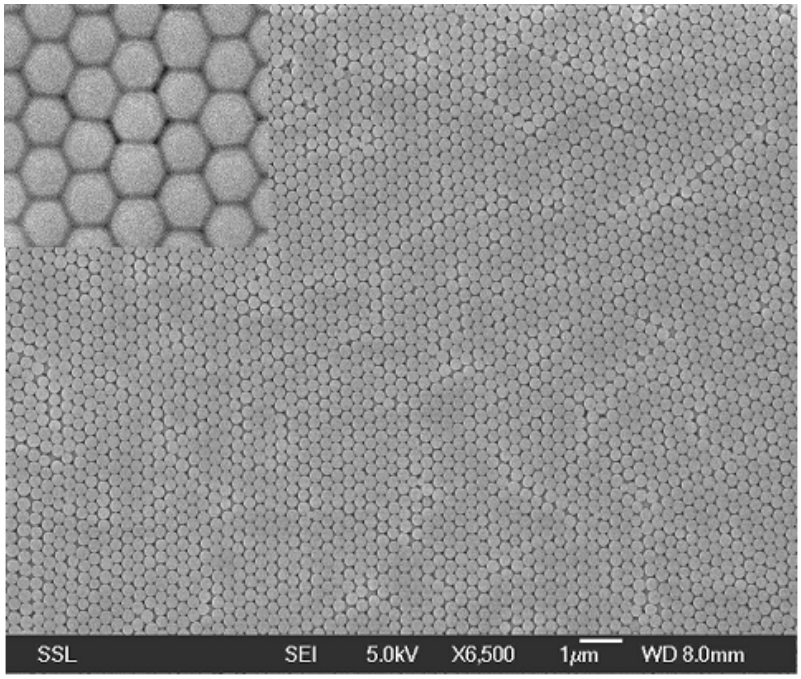

(a)

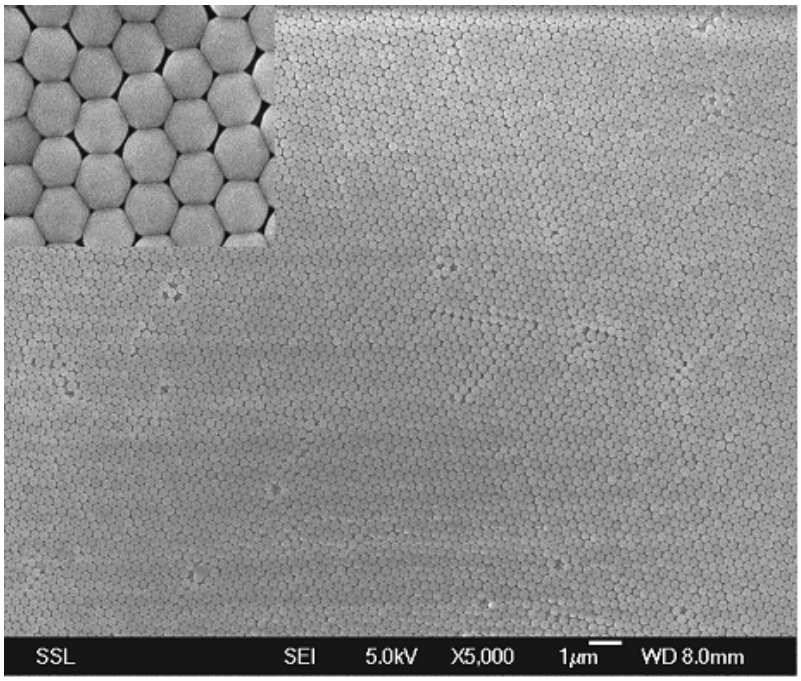

(b)

Figure 4.1. (a) SEM image of colloidal crystal made from original silica particles; the size of the particles is 290 nm; (b) SEM image of colloidal crystals assembled from heat-treated silica particles. The particles were heated at 650^0C for 2 hours prior to assembly of the opal. The size of the particles is 272 nm.

The decrease in size can be attributed to the evaporation of water, followed by the elimination of pores in silica spheres during heating. The shrinkage was irreversible and not affected by the solvent. In particular, the refractive index of the heat-treated silica is smaller than that of original silica and shows an unusual dependence upon T based on the results of similar work recently done by D. J. Norris and co-works. The refractive index first decreases; then at T above 400^0C, it increases, approaching the refractive index of fused quartz. [13]

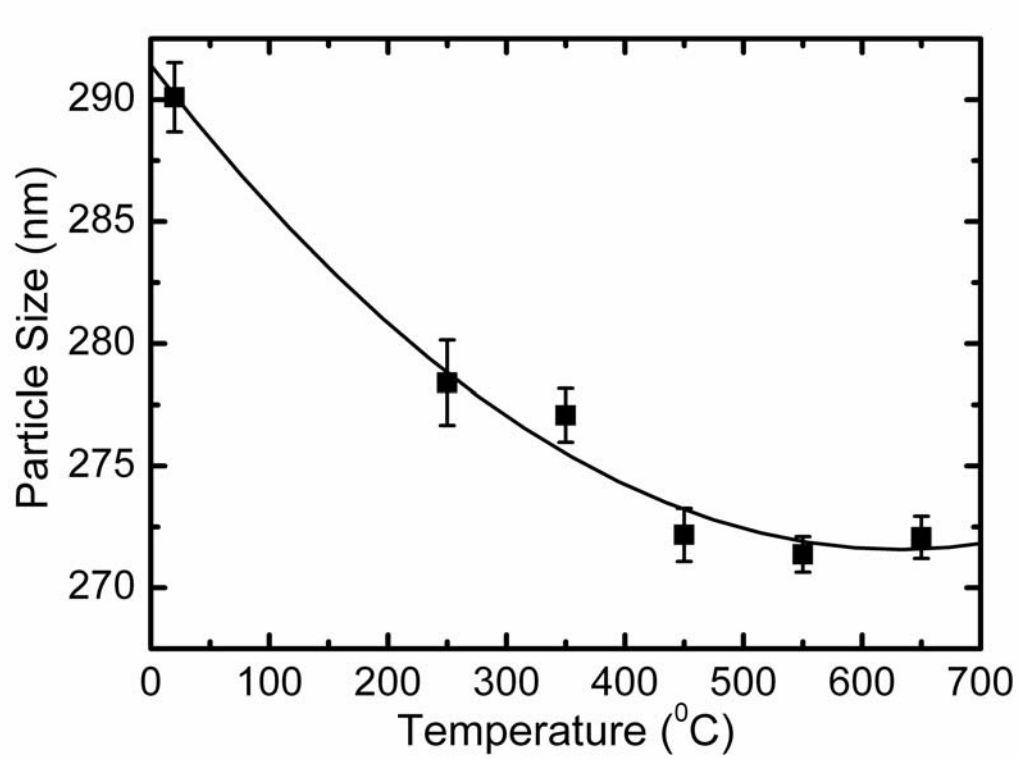

Figure 4.2. A plot of silica particle size verus the pre-heating temperature.

Figure 4.3 shows the reflectance spectra of silica colloidal crystals from original and heat-treated silica spheres. A stop bandgap for each sample can be observed. The mid-gap position of colloidal crystals of original silica spheres is at 603.5±1.2nm, and that of colloidal crystals of silica spheres pre-heating at 250^0C, 350^0C, 450^0C, 550^0C and 650^0C

is 602.5±1.2nm, 592.5±1.1nm, 594.5±1.1nm, 602.0±1.2nm, and 615.5±1.4nm, respectively. The spectrum that corresponds to the colloidal crystal from particles heat-treated at 650^{0}C shows unusually broad peak. This may be due to more cracks formed in the colloidal crystal resulted from the higher deviation of the particle size after heating treatment at such high temperature. Figure 4.4 gives a plot of the mid-gap position versus the pre-heating temperature. The mid-gap position first shifts towards shorter wavelengths; then at T above 350^{0}C, it shifts towards longer wavelengths. When T increases to 650^{0}C, the mid-gap position is even larger than that of colloidal crystal of original silica spheres.

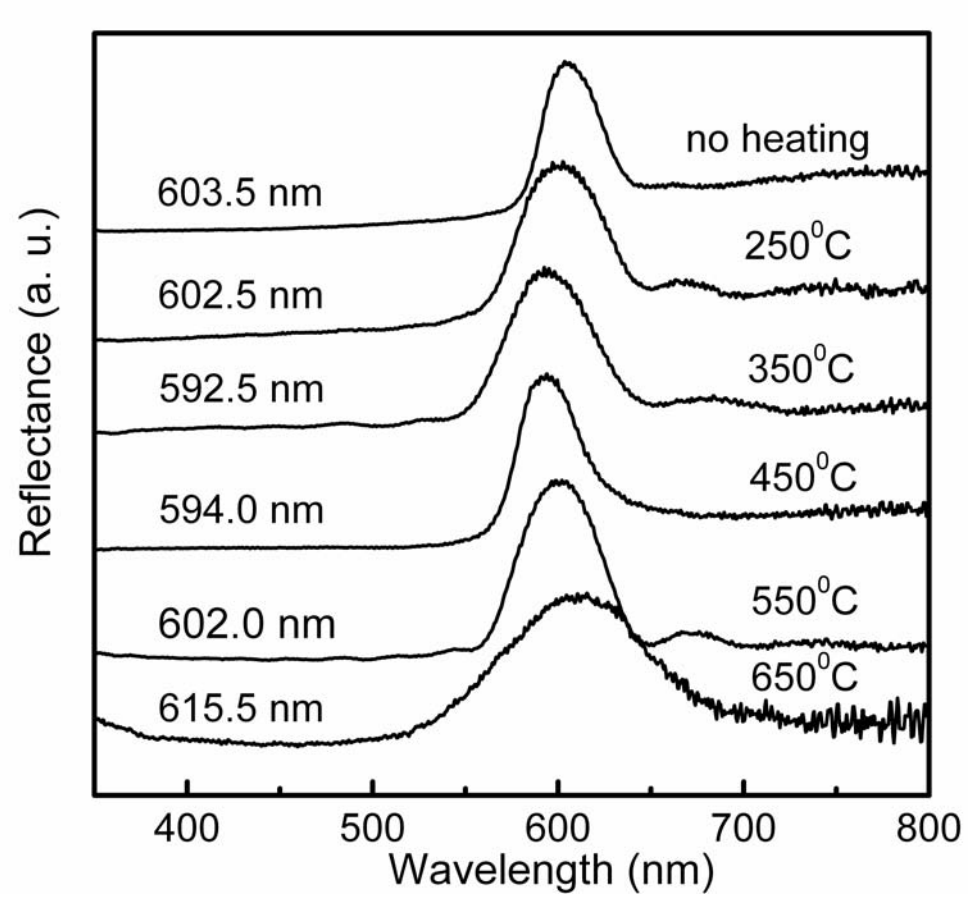

Figure 4.3. Reflectance spectra of silica colloidal crystals from original and heat-treated silica spheres.

A crystalline lattice of colloidal particles diffracts light according to the Bragg equation:[14]

$$\lambda_{\min} = 2(2/3)^{1/2} D(n^2 - \sin^2\theta)^{1/2} \quad (4.1)$$

where $\lambda_{\min}$ is the wavelength of the diffraction peak known as middle stop bandgap position; D is the diameter of the particles; θ is the angle between the incident light and the normal to the diffraction planes (at normal incidence, $\theta = 0$); and n is the mean refractive index of this crystalline lattice. As a good approximation, n can be calculated using the following formula:

$$n = n_p f + n_m(1 - f) \quad (4.2)$$

where n_p is the refractive index of colloidal particles; f is the volume fraction occupied by the particles; and n_m represents the refractive index of air in the crystals. In this case, $n_m = 1$, and the volume fraction was $f = 0.74$ for all the samples since the spherical shape of the silica particles were maintained during the pre-heating treatments. Therefore, in our case, the Bragg equation can be rewritten as:

$$\lambda_{\min} = (1.48 n_p + 0.52)\sqrt{2/3} D \quad (4.3)$$

From Equation (4.3), it can be seen that the mid-gap position is determined by the size and the refractive index of the silica particles. In our experiments, the size became smaller and then approached a constant value with the preheating temperature, and this change in size may lead to the blue shift of $\lambda_{\min}$; while the refractive index first decreases; and then at T above 400^0C, it increases, and this change in refractive index first result in the blue shift and then the red shift. Therefore the mid-gap position blue shifted when T is below 400^0C. When T is above 400^0C, the competition between the two effects can explain the results in Figure 4.4.

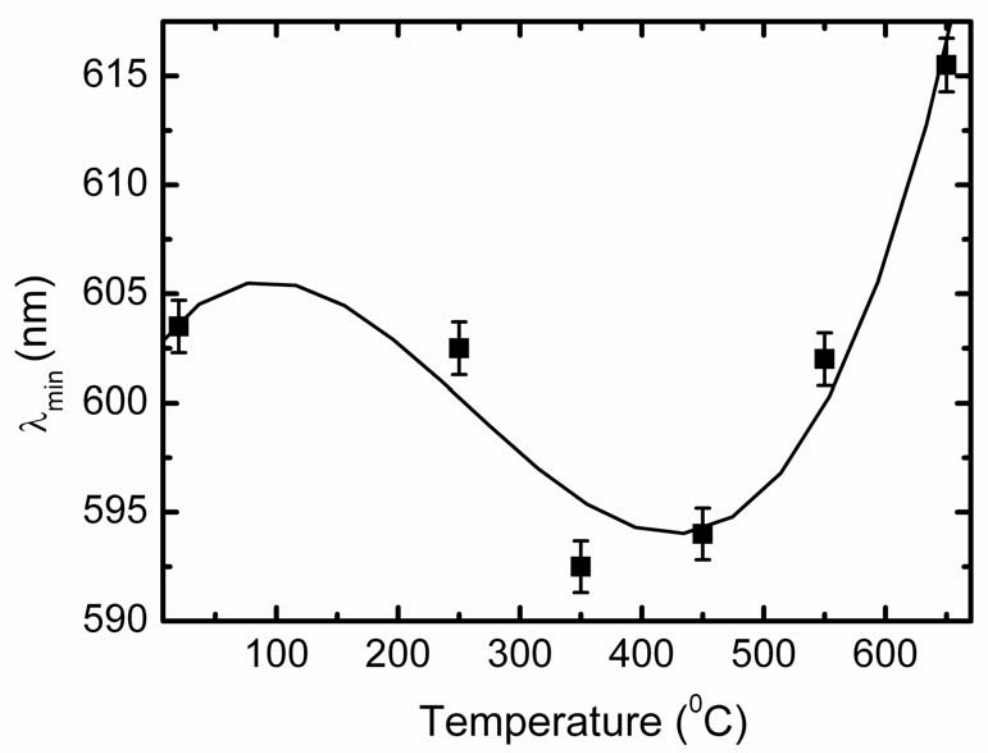

Figure 4.4. A plot of the mid-gap position versus the preheating temperature.

4.4 Conclusions

In summary, we have demonstrated an efficient method for fine-tuning the bandgap properties of three-dimensional PBG crystals made from monodispersed silica spheres. In this method, the silica colloids were heated at temperatures in the range of 250-650^{0}C prior to formation of colloidal crystals and then redispersed into deionized water for the fabrication of crystals. Compared to the mid-gap position of the crystal from original silica spheres, that of samples from heat-treated silica spheres first blue shifted and then red shifted with increasing the pre-heating temperature due to the change of the silica particle size and refractive index. This approach may enable us to obtain PBG crystals

with desired properties in any specific spectral region and would have potential application in integrated optics.

References

[1] E. Yablonovitch, *Phys. Rev. Lett.* **58**, 2059 (1987).

[2] S. John, *Phys. Rev. Lett.* **58**, 2486 (1987).

[3] J. D. Joannopoulous, R. D. Meade, J. N. Winn, *Photonic Crystals*, Princeton University Press, Princeton, NJ (1995).

[4] Yu. A. Vlasov, M. Deutsch, and D. J. Norris, *Appl. Phys. Lett.* **76**, 1627 (2000).

[5] Cefe Lopez, *Adv. Mater.* **15**, 1679-1704 (2003).

[6] Sang Hyun Park, Dong Qin, and Younan Xia, *Adv. Mater.* **10**, 1028-1032 (1998).

[7] Hailin Cong and Weixiao Cao, *Langmuir* **19**, 8177-8181 (2003).

[8] Sang Hyuk Im, Mun Ho Kim, and O Ok Park, *Chem. Mater.* **15**, 1797-1802 (2003).

[9] Hernan Míguez, Francisco Meseguer, Cefe López, Alvaro Blanco, Jose S. Moya, Joaquín Requena, Amparo Mifsud, and Vicente Fornes, *Adv. Mater.* **10**, 480-483 (1998).

[10] Byron Gates, Sang Hyun Park, and Younan Xia, *Adv. Mater.* **12**, 653-656 (2000).

[11] Younan Xia, Byron Gates, Yadong, Yin, and Yu Lu, *Adv. Mater.* **12**, 693-713 (2000).

[12] Hiroshi Fudouzi, *Journal of Colloidal and Interface Science* **275**, 277-283 (2004).

[13] A. A. Chabanov, Y. Jun, and D. J. Norris, *Appl. Phys. Lett.* **84**, 3573-3575 (2004).

[14] A. Richel, N. P. Johnson, D. W. McComb, *Appl. Phys. Lett.* **76,** 1816 (2000).

Chapter 5 Fabrication and Characterization of Surfactant-assisted TiO_2 Photonic Crystals

5.1 Introduction

Since their proposal in 1987, periodic dielectric structures exhibiting a complete photonic band gap (PBG) have gained considerable attention.[1] They consist of a low absorption material having a three dimensional spatially periodic dielectric lattice, with a lattice constant of the order of the wavelength of light (about 500nm). Bragg reflections occur on lattice planes which forbid a particular range of wavelengths from propagating in the material. A photonic band gap occurs when a range of wavelengths is forbidden for every state of polarization and propagation direction.[2] Photonic crystals have potential use in various applications such as waveguides, optical filters, switches, high-density magnetic data storage devices, and chemical and biochemical sensors.[3] To exhibit such a PBG the photonic crystal has to be made of topologically interconnected materials with a large refractive index contrast (RIC). Theoretical studies indicate that the minimum contrast between the refractive indices at which a complete gap (between the eighth and ninth bands) is formed depends on the structural type and varies from 1.9 for a layered structure, through ~2.1 for a diamond structure, to ~2.8-2.9 for a face centered cubic inverse opal structure.[4]

Colloidal crystals assembled from highly charged polystyrene or silica spheres have been known for a long time to produce Bragg diffraction of light in the optical region.

However, colloidal crystals do not exhibit full bandgaps due to the relatively low dielectric contrast that can be achieved for these materials. Computational studies have suggested that a porous material consisting of an opaline lattice of interconnected air balls (embedded in an interconnected matrix with a higher refractive index) should give rise to a complete gap in the 3D photonic band structure.[5] Optimum photonic effects require the volume fraction of the matrix material to fall anywhere in the range of 20±30 %. Although such a 3D structure can be built up layer by layer through conventional microlithographic techniques, it has been very difficult to achieve that goal when the feature size becomes comparable to the wavelength of visible light.[6] Processing difficulties have also limited the formation of such 3D structures with more than a few layers, or from materials other than those currently employed in microelectronics. An alternative approach is based on template-directed synthesis against colloidal crystals. This method is attractive because the periodicity of this system can be conveniently tuned and a wide variety of materials with relatively high refractive indices can be easily incorporated into the procedure.

The most promising candidates for the matrix seem to be some wide bandgap semiconductors such as diamond, II-VI semiconductors (e.g., CdS and CdSe), titania, and tin dioxide because they have a refractive index higher than 2.5 and are optically transparent in the visible and near-IR region.[7] Other semiconductors with strong absorption in the visible region (such as Si and Ge) can be applied to the near-IR

regime. Since the first demonstration by Velev et al. in 1997, many advances have recently been made in this area.[8] For instance, Vos and co-workers have demonstrated the fabrication with polycrystalline titania (anatase) by using a sol-gel process and also measured the reflectance spectrum of this crystal.[9] Baughman and co-workers have incorporated chemical vapor deposition (CVD) into this procedure and generated inverse opals containing different forms of carbon.[10] Norris and co-workers and Braun and Wiltzius were able to obtain 3D periodic structures from II-VI semiconductors such as CdS and CdSe, albeit no optical measurement was presented in their publications.[11] Stein and co-workers, Velev et al., and Colvin and co-workers also fabricated highly ordered 3D porous materials from metals that might display interesting photonic properties.[12] Pine and co-workers and Subramanian et al. have fabricated inverse opals of titania by filling the void spaces among colloidal spheres with slurries of nanometer-sized titania particles.[13] They also observed stop bands (between the second and third bands) for these 3D porous materials made of rutile- and anatasephase titania. Despite these advances, a definitive signature of the existence of a complete photonic bandgap is still missing for these 3D porous materials. Part of the reason lies on the fact that the filling of the void spaces was not complete in most cases and the resulting materials might not be dense enough to acquire a refractive index close to that of the bulk materials.

In our experiments, we fabricated TiO_2 photonic crystals by using colloidal crystal templating method. Polystyrene (PS) colloidal crystals were used as templates and a

solution of Tetra-Propoxy-Titane (TPT) in ethanol was used as the infiltration material. Their structures and optical properties were studied with scanning electron micrograph (SEM) and micro-FTIR, respectively. The effect of surfactant on infiltration process was explored by adding SDS in TPT solution.

5.2 Experiments

We used colloidal crystal templating method [14] to fabricate crystals of air spheres in titania, producing photonic crystals with a high refractive index. The photonic crystals were prepared as follows. The templates were firstly assembled from a self-organizing system. The desired solid material was then infiltrated into the voids of the template. Finally, the macro-porous samples were obtained by removing the original templates by calcination or wet etching. The general procedure is shown in Figure 5.1.

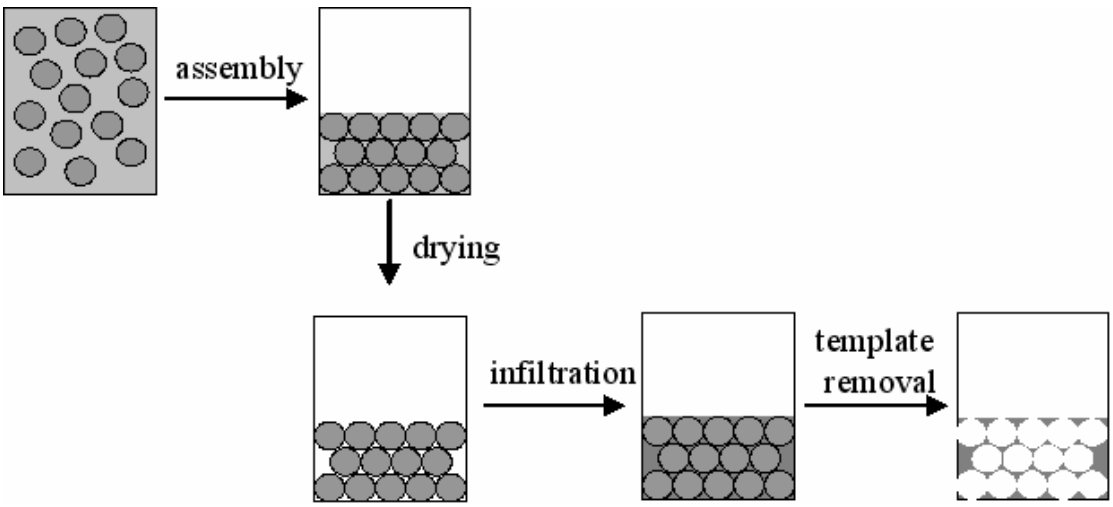

Figure 5.1. Schematic illustration of colloidal crystal templating.

Firstly, PS colloidal crystals used as templates were assembled from PS colloids by sedimentation. Monodispersed PS colloidal spheres with diameter of 300nm were

used as received from the supplier (Duke Scientific). The colloidal suspensions were loaded on thin cleaned glass plates or silicon wafers. As solvent evaporated, PS colloidal crystals (opals) were obtained. Slow evaporation is necessary to minimize the number of cracks that appear in the opals.

Secondly, the voids in the opals were filled with TPT solution by precipitation from a liquid–phase chemical reaction. The precursor liquid penetrates the voids in the opal by capillary forces. The TPT solution has high reactivity to water and reacts with water from the atmosphere when it is infiltrated into the opals. We repeated the cycle of penetration, reaction, and drying up to three times (depending on the concentration of TPT) to ensure that the voids in the opal were sufficiently filled. In order to investigate the effect of surfactant on the infiltration process, a PS colloidal crystal was filled with the mixture of TPT and (Dodecyl sulfate, sodium salt) SDS solution.

Finally, PS particles were removed by calcination. Calcinations is the common method in the preparation of inorganic porous materials made form organic templates.[9] The samples were slowly heated (5^0C per minute) to 450^0C and kept heated for 2 hours. The PS particles were gasified and burned during the heating process. Photonic crystals of air spheres embedded in TiO_2 were thus obtained.

The inverse opals were observed by SEM for determining the structure. Because cracks exist inevitably in inverse opals and the typical size of a single domain crystal

is about 50-100μm, the common UV-Vis spectrometer with much larger beam size can not proved the photonic bandgaps in inverse opals, Herein we also fabricated an inverse opal from PS particles with a diameter of 0.99μm and studied its optical properties using micro-FTIR.

5.3 Results and Discussion

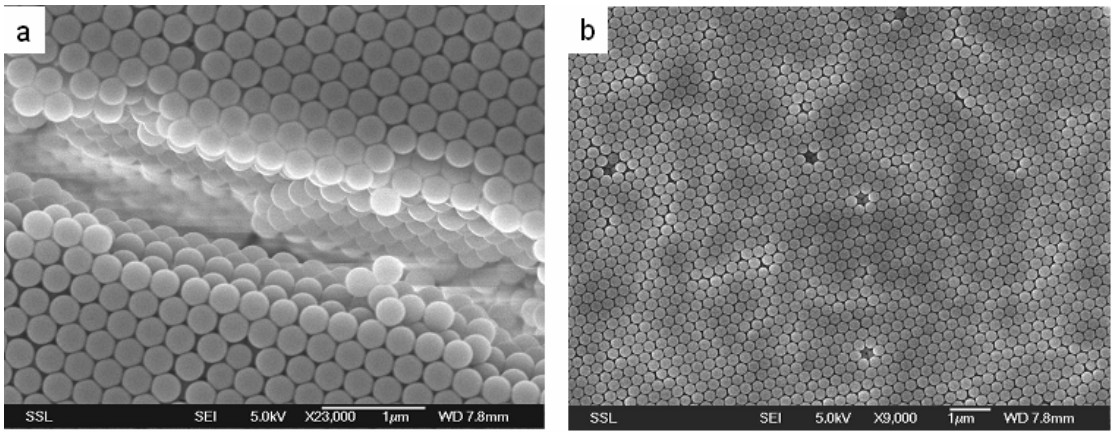

Figure 5.2. SEM images of a PS colloidal crystal. (a) Oblique view along a crack; (b) hexagonal array observed in the colloidal crystal.

Figure 5.2 shows SEM images of a colloidal crystal assembled from PS particles with a diameter of 300nm by sedimentation. It is clear that the resulting template has the fcc structure with (111) plane parallel (hexagonal array) to the substrate. From the point defects in Figure 5.2b, we can see that the upper layer of the crystal possesses the same array as that of the layer just below it. That is, in the formation of a colloidal crystal, the array fashion of the colloids has transitivity, and the upper layer is always the replica of the underside layer. The crystal has a high degree of order, but local defects can also be observed, such as point defects (Figure 5.2b), stacking faults, etc. In addition, cracks formed in the crystal during drying process (Figure 5.2a). Due to

the macroscopic size of sedimented opals, colloidal crystals are polycrystalline and the typical size of a single crystalline is about 100 μm.

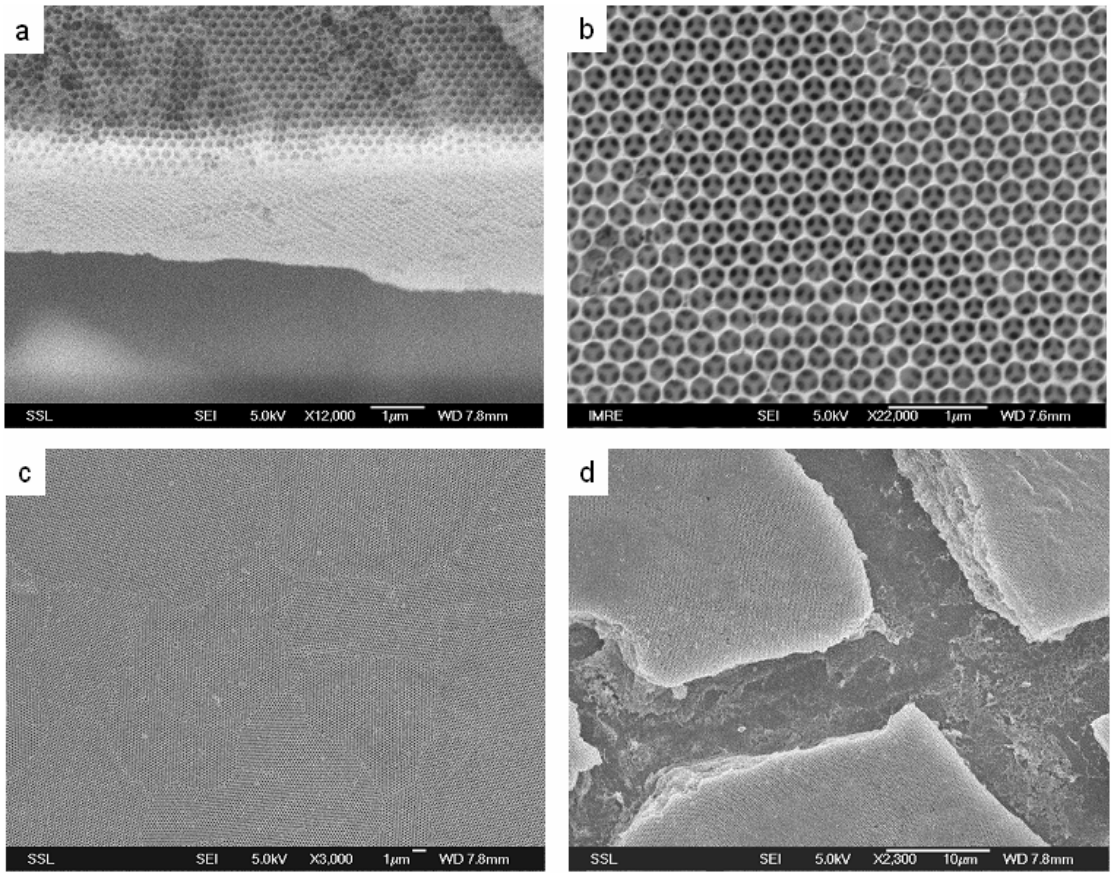

Figure 5.3. SEM images of a TiO_2 photonic crystal. (a) Oblique view; (b) view in large magnification; (c) view in small magnification; (d) cracks in the crystal. Its template was assembled form PS particles with a diameter of 300nm.

Figure 5.3 shows SEM images of a TiO_2 photonic crystal. The resulting macroporous structures show an ordered hexagonal pattern of spherical holes in the TiO_2 matrix. The next lower layer of air spheres is visible in the SEMs, as well as the holes that connect each air sphere to its nearest neighbors in the next layer. Both the TiO_2 structure and the air spheres are connected, which is favorable to realize band gaps in photonic crystals.[9] It is shown that the inverse opals have lattice parameters that are

about 33% less than those of the original opals. Such large shrinkage formed during heating the sample at elevated temperature. Additionally, drying at elevated temperature invariably involves a crack formation process. Drying involves a contraction that does not occur in the supporting substrate, which can only be accommodated by the creation of cracks, as defects accommodate lattice mismatch in epitaxially grown materials. The sample is polycrystalline and each domain consists of many single crystals.

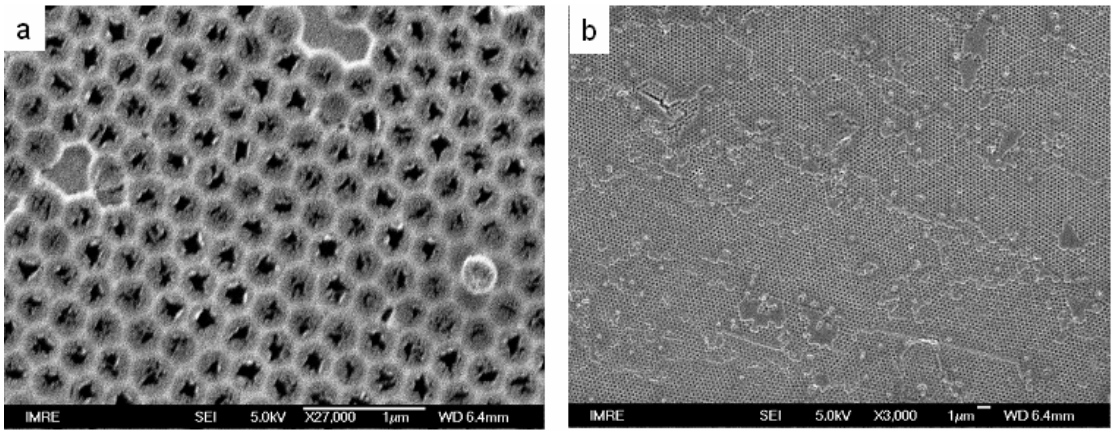

Figure 5.4. SEM images of a TiO_2 photonic crystal produced using the mixture of TPT and SDS solution as the infiltration material. a) View in large magnification; b) view in small magnification. Its template was assembled form PS particles with a diameter of 300nm.

Figure 5.4 shows SEM images of a TiO_2 photonic crystal, which was produced by using the mixture of TPT and SDS solution as the infiltration material, while other fabricating conditions were kept the same as that produced in the absence of SDS. The crystal has the same symmetry compared to that formed in the absence of SDS. But there are thin layers (Figure 5.4b) of TiO_2 on some areas of the sample surface and the air spheres in the top layer have relatively small or no openings (Figure 5.4b).

We may conclude that the addition of SDS might lead to tight coating of TiO_2 on the PS microspheres in the infiltration process and thus results in the relatively small or no openings in the air spheres.

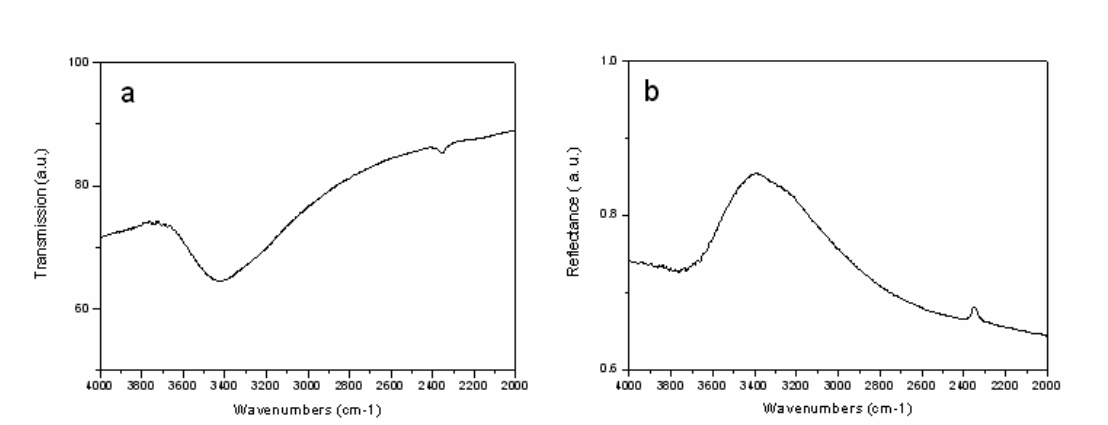

Figure 5.5. Micro-FTIR transmission (a) and reflectance (b) spectra of a TiO_2 inverse opal. The template of the inverse opal was assembled form PS particles with a diameter of 0.99μm.

Figure 5.5 illustrates the transmission and reflectance spectra measured at normal incidence to the substrate using micro-FTIR. From the images, we can see that there is broad peak at 2.94μm ($\frac{1}{\lambda} = 3400\,\mathrm{cm}^{-1}$), which is corresponding to the stop bandgap. According to Bragg equation: [9]

$$m\lambda_{\min} = 2d_{hkl}(n^2 - \sin^2\theta)^{1/2} \tag{5.1}$$

where m is the order of diffraction; $\lambda_{\min}$ is the wavelength of the diffraction peak; d_{hkl} is the spacing between (*hkl*) planes and $d_{hkl} = \sqrt{2/3}D$, where D is the diameter of the particles; θ is the angle between the incident light and the normal to the diffraction planes (at normal incidence, $\theta = 0$); and n is the mean refractive index of this crystalline lattice. As a good approximation, n can be calculated using the following formula:

$$n = n_a f + n_{TiO_2}(1 - f) \tag{5.2}$$

where n_a is the refractive index of air spheres; f is the volume fraction occupied by the air spheres; and n_{TiO_2} represents the refractive index of titania. Through calculation, the mean refractive index of the inverse opal should be 1.47. The diffraction peak should be at 2.38μm corresponded to a lattice spacing of 0.812μm between the (111) planes perpendicular to the incident light. This is in reasonable agreement with the experimental value of 2.94μm. The difference between the experimental value and the theoretical value may be due to the defects, cracks and the difference between the refractive index of nanostructure titania and that of bulk titania. Therefore, the presence of stop band-gap was proved experimentally using micro-FTIR.

5.4 Conclusions

In summary, well-ordered TiO_2 photonic crystals were fabricated by using colloidal crystal templating method. The crystals have the structure of an fcc lattice with (111) plane parallel to the surface of supporting substrates. The single-domain area of the crystals is quite large so that their stop bandgap can be proved experimentally. The existence of stop bandgaps confirmed the high quality of the crystals. The addition of SDS in the infiltration material might lead to tight coating of TiO_2 on the PS microspheres in the infiltration process, but its effect on the reflectance and transmission spectra of the crystals is invisible.

References

[1] Kurt Busch and Sajeev John, *Phys. Rev. E* **58**, 3896-3908 (1998).

[2] A. Richel, N. P. Johnson, and D. W. McComb, *Appl. Phys. Lett.* **76**, 1816-1818 (2000)

[3] Sang Hyuk Im, Mun Ho Kim, and O Ok Park, *Chem. Mater.* **15**, 1797-1802 (2003)

[4] Younan Xia, Byron Gates, Yadong Yin, and Yu Lu, *Adv. Mater.* **12**, 693-713 (2000)

[5] K. Busch, S. John, *Phys. Rev. E* **58**, 3896 (1998).

[6] S. Y. Lin, J. G. Fleming, D. L. Hetherington, B. K. Smith, R. Biswas, K. M. Ho, M. M. Sigalas,W. Zubrzycki, S. R. Kurtz, J. Bur, *Nature* **394**, 251 (1998).

[7] L. I. Berger, *Semiconductor Materials*, CRC Press, Boca Raton, FL (1997).

[8] O. D. Velev, T. A. Jede, R. F. Lobo, A. M. Lenhoff, *Nature* **389**, 447 (1997).

[9] a) J. E. G. J. Wijnhoven, W. L. Vos, *Science* **281**, 802 (1998). b) M. S. Thijssen, R. Sprik, J. E. G. J. Wijinhoven, M. Megens, T. Narayanan, A. Lagendijk, W. L. Vos, *Phys. Rev. Lett.* **83**, 2730 (1999).

[10] A. A. Zakhidov, R. H. Baughman, Z. Iqbal, C. Cui, I. Khayrullin, S. O. Dantas, J. Marti, V. G. Ralchenko, *Science* **282**, 897 (1998).

[11] a) Y. A. Vlasov, N. Yao, D. J. Norris, *Adv. Mater.* **11**, 165 (1999). b) P. V. Braun, P. Wiltzius, *Nature* **402**, 603 (1999).

[12] a) H. Yan, C. F. Blanford, B. T. Holland, M. Parent, W. H. Smyrl, A. Stein, *Adv. Mater.* **11**, 1003 (1999). b) O. D. Velev, P. M. Tessier, A. M. Lenhoff, E. W.

Kaler, *Nature* **401**, 548 (1999). c) P. Jiang, J. Cizeron, J. F. Bertone, V. L. Colvin, *J. Am. Chem. Soc.* **121**, 7957 (1999).

[13] a) G. Subramanian, V. N. Manoharan, J. D. Thorne, D. J. Pine, *Adv. Mater.* **11**, 1261 (1999). b) G. Subramania, K. Constant, R. Biswas, M. M. Sigalas, K.-M. Ho, *Appl. Phys. Lett.* **74**, 3933 (1999).

[14] Arnout Imhof, *Three-Dimensional Photonic Crystals Made from Colloids*, 424-446.

Chapter 6 Conclusion

Photonic crystals and photonic bandgap materials have been the subjects of great interests, both theoretically and experimentally.[1] Their periodic dielectric structures are designed to control the propagation of electromagnetic (EM) waves by defining allowed and forbidden energy gaps in the photon-dispersion spectrum. The absence of EM modes inside the structures gives rise to distinct optical phenomena such as the inhibition of spontaneous emission [2] and the strong localization of light [3]. Photonic crystals have been proposed for a large number of applications such as efficient microwave antennas, zero-threshold lasers, low-loss resonators, optical switches, and miniature optoelectronic components such as microlasers and waveguides. The most useful applications would occur at near-infrared or visible wavelengths.[4-9]

One of the promising techniques of fabricating three–dimensional photonic crystals with a photonic bandgap is the templating of self-assembled colloidal crystals.[10, 11] Though colloidal crystals show pseudo-photonic bandgaps, they have been widely studied due to the ease of growing a 3D periodic structure. Also they offer a simple and easily prepared model system to experimentally probe the photonic band diagrams of certain type of three-dimensional periodic structure. Macroporous ordered structures with a wider photonic bandgap can be fabricated by filling the voids in the colloidal crystal templates with materials possessing high refractive index, followed by the removal of the original colloidal crystal materials.[12, 13]

Although the photonic crystals fabricated from the colloids are studied intensively recently, some bottlenecks exist, for example, defects, disorders and cracks formed invariably in the crystals. Investigations related to the array fashion of the particles and studies on the control of the photonic crystal properties of colloidal crystals are very limited. To obtain high-quality photonic crystals with fewer defects, disorders and cracks, which can meet the requirement for producing the photonic device, we fabricated colloidal crystals by optimizing fabrication conditions. The effects of surfactants on the array fashion of the particles and the effects of pre-heating treatment on the photonic bandgap properties of silica colloidal crystals were also investigated. Furthermore, surfactant-assisted TiO_2 photonic crystals were fabricated, and their structures and optical properties were studied by SEM and Micro-FTIR, respectively. The main results are described as follows.

Colloidal crystals were assembled from polystyrene and silica colloidal particles using modified sedimentation and vertical deposition methods. The crystals have the structure of fcc lattice. The defects, disorders and cracks in the crystals were greatly reduced by optimizing the crystallization temperature and the concentration of the colloidal particles. Reflectance and transmission spectra measured at the normal incidence to the sample surface with UV-Vis spectrometer demonstrate that stop bandgaps exist in the colloidal crystals.

The effects of surfactants on the structures of colloidal crystals were investigated by

fabricating colloidal crystals in the presence of different surfactants with different concentrations by sedimentation. The addition of surfactants affects the array fashion and is favorable to form a square array due to the change of interaction between the particles.

The effects of pre-heating treatment on the photonic bandgap properties of silica colloidal crystals were also explored by pre-heating the silica colloids at temperatures in the range of 250-650^{0}C prior to assembly of colloidal crystals. Compared to the mid-gap position of the crystal from original silica spheres, that of crystals from heat-treated silica spheres first blue shifted and then red shifted with increasing the pre-heating temperature. The shift in the mid-gap position resulted from the change of the silica particle size and refractive index.

Well-ordered TiO_2 photonic crystals were fabricated using polystyrene colloidal crystal templating. The inverse opals had the same structure as the colloidal crystals. The TiO_2 photonic crystals are polycrystalline and the typical size of a single crystal is about 100μm. Micro-FTIR transmission spectra confirmed the existence of stop bandgaps in the crystals. In addition, SEM results show that the addition of SDS might lead to tight coating of TiO_2 on the PS microspheres in the infiltration process.

References

[1] M. Hanack, M. Lang, *Adv. Mater.* **6**, 819 (1994).

[2] U. Drechsler, M. Hanack, *Comprehensive Supramolecular Chemistry*, Vol. 9 (Eds: J. L. Atwood, J. E. D. Davis, D. D. MacNicol, F. Vögtle), Pergamon, Oxford, UK 1996, p. 283.

[3] N. B. McKeown, *Phthalocyanine Materials: Synthesis, Structure and Function, Chemistry of Solid State Materials*, Vol. 6, Cambridge University Press, Cambridge, UK 1998.

[4] P. Gregory, *High-Technology Applications of Organic Colorants*, Plenum, New York, 1991, p 59.

[5] P. N. Prasad, D. J. Williams, *Introduction to Nonlinear Optical Effects in Molecules and Polymers*, Wiley, New York 1991, p 243.

[6] H. S. Nalwa, *Nonlinear Optics of Organic Molecules and Polymers* (Eds: H. S. Nalwa, S. Miyata), CRC Press, Boca Raton, FL 1997, p 611.

[7] H. S. Nalwa, J. S. Shirk, *Phthalocyanines: Properties and Applications*, Vol. 4 (Eds: C. C. Leznoff, A. B. P. Lever), VCH, Weinheim, Germany 1996, p 79.

[8] J. W. Perry, *Nonlinear Optics of Organic Molecules and Polymers* (Eds: H. S. Nalwa, S. Miyata), CRC Press, Boca Raton, FL 1997, p 813.

[9] J. S. Shirk, R. G. S. Pong, F. J. Bartoli, A. W. Snow, *Appl. Phys. Lett.* **63**, 1880 (1993).

[10] a) J. W. Perry, K. Mansour, I. Y. S. Lee, X. L. Wu, P. V. Bedworth, C. T. Chen, D. Ng, S. R. Marder, P. Miles, T. Wada, M. Tian, H. Sasabe, *Science* **273**, 1533

(1996). b) J. S. Shirk, R. G. S. Pong, S. R. Flom, H. Heckmann, M. Hanack, J. *Phys. Chem. A* **104**, 1438 (2000).

[11] G. Y. Yang, M. Hanack, Y. W. Lee, Y. Chen, M. K. Y. Lee, D. Dini, *Chem. Eur. J.* **9**, 2758 (2003).

[12] S. M. O'Flaherty, S. V. Hold, M. J. Cook, T. Torres, Y. Chen, M. Hanack, W. J. Blau, *Adv. Mater.* **15**, 19 (2003).

[13] a) G. De la Torre, P. Vazquez, F. Agullo-Lopez, T. Torres, *Chem. Rev.* **104**, 3723 (2004). b) M. Calvete, G. Y. Yang, M. Hanack, *Synth. Met.* **141**, 231 (2004).

Appendices

List of publications

Paper submitted

Yanhua Wang, Ke-Qin Zhang and Xiang-Yang Liu “Effects of Pre-heating Treatment on Photonic Bandgap Properties of Silica Colloidal Crystals” (submitted to Langmuir).

Conferences

Yanhua Wang, Xiang-Yang Liu and Keqin Zhang, “Fabrication of TiO2 Photonic Crystals from Colloidal Assembly”, ICMAT 2005, Singapore.

Yanhua Wang, Xiang-Yang Liu and Keqin Zhang “Fabrication of Inverse opals by Surfactant-Assisted Template”, Japan-Singapore Symposium on Nanoscience & Nanotechnology (01-04 November, 2004, Singapore).